Master´s thesis

Optimal integration of flexible loads and PV power generation in an isolated grid

Martin Burkhard

November 2015

Supervisor: Dipl.-Wirt.-Ing. Hannes Schwarz

Reviewer: Prof. Dr. Wolf Fichtner

Co-supervisor: Dr. Thomas Walter, easy smart grid GmbH

Institute for Industrial Production

Department of Economics and Management

Karlsruhe Institute of Technology

Abstract

Energy supply of isolated communities is mostly achieved by diesel generators and fossil fuels. This leads to high electricity prices with a high dependency on expensive fuel and the global oil price. As renewable energies are becoming more and more cost competitive, the interest of isolated communities in renewable energies rises. The additional integration of flexible loads can lead to synergy effects and thus further increase the interest in renewables.

In order to answer the economic and functional interaction of PV power generation and flexible loads in isolated grids, a mathematical optimization model for an isolated grid and its system components is developed in the General Algebraic Modeling System as a linear program, respectively mixed integer linear program. The objective of the model is the minimization of the annual total costs for the energy supply system and the model is solved with IBMS`s Cplex solver. As flexible loads, a desalination process and a battery storage system is considered. Several scenarios for the integration of PV power generation and the flexible loads are defined and studied. Furthermore, a decentralized integration approach of a flexible load with a price signal is conducted and compared. The uncertain parameters are studied and the most important ones are identified.

The main outcomes are:are the integration of PV power in an isolated grid results in lower total cost for the energy supply. The integration of flexible loads either results in a better utilization of PV power or in a higher penetration of PV powerand thus also in lower total cost for the energy supply. Battery storage systems are still too expensive to be beneficial from an economic point of view. The decentralized integration approach of the flexible load with a price signal shows different operational characteristics, but the resulting key figures are comparably similar. The most important uncertain parameters are all related to the diesel generator, as the main part of electricity is still diesel generated.

Declaration of Authorship

I hereby certify that this thesis has been composed by me and is based on my own work, unless stated otherwise. No other person's work has been used without due acknowledgement in this thesis. All references and verbatim extracts have been quoted, and all sources of information, including graphs and data sets, have been specifically acknowledged.

Date: 11.11.2015 **Signature:** Martin Burkhard

Contents

List of Figures

List of Tables

List of abbreviations and nomenclature

Abbreviation

AC	Alternate current	
BS	Battery storage	
CPP	Critical peak pricing	
DC	Direct current	
DG	Diesel generator	
DSM	Demand side management	
ICT	Information commmunication technology	
GAMS	General Algebraic Modeling System	
LCOE	Levelized cost of energy	\$/kWh
lp	Linear program	
milp	Mixed integer linear program	
PV	Photovoltaics	
RO	Reverse osmosis	
RTP	Real-time pricing	
TERM	Tonga Energy Road Map	
TOU	Time-of-use rates	
TPL	Tonga Power Ltd	
TWB	Tonga Water Board	
WS	Water storage	

Parameter	**Description**	
A^{BS}	Annuity factor of the battery storage	
A^{PV}	Annuity factor of the PV system	
C^{BS}	Price of a battery unit	\$/unit
C^{PV}	Price of one kW_P PV power	\$/kW_P
C^{diesel}	Price of one liter of diesel fuel	\$/l
$E^{BS,cap}$	Power capacity of one battery unit	kW
E_t^{demand}	Static electricity demand	kWh
$E_t^{PV1kW_P}$	Energy generated by a PV System with 1 kW_P	kWh/ kW_P
$F^{DG,A}$	Conversion factor of the DG	l/kWh
$F^{DG,B}$	Conversion factor of the DG	l/kWh
$F^{DG,C}$	Conversion factor of the DG	l/kW
F^{RO}	Conversion factor of the RO plant	kWh/m³
I	Interest rate	
$L^{BS,dd}$	Deep discharging rate of the battery storage	
$L^{BS,rte}$	Round-trip efficiency of the battery storage	

$L^{BS,sdl}$	Self-discharging losses of the battery storage	
L^{DG}	Additional fuel consumption of the DG	
L^{RO}	Infinitesimal loss factor of the RO plant	
LT^{BS}	Life time of the battery storage	Years
LT^{PV}	Life time of the PV system	Years
P_t^{RO}	Price signal for the decentralized control approach	$
RP^{DG}	Rated power of the DG	kW
RP^{RO}	Rated power of the RO system	kW
$S^{BS,cap}$	Energy capacity of one battery unit	kWh
$S^{WS,max}$	Maximal water storage capacity in days	Days
T_t	Temperature for the PV system	°C
W_t^{demand}	Water demand for the RO plant	m³

Variable	**Description**	
b_t^{DG}	Binary variable for the DG	
b_t^{RO}	Binary variable for the RO plant	
$cost^{BS}$	Cost of the battery storage	$
$cost^{DG}$	Cost of the DG	$
$cost^{PV}$	Cost of the PV system	$
$cost^{total}$	Total costs of the year	$
$diesel_t$	Consumed diesel fuel	l
e_t^{BS}	Energy going/coming to/from the BS system	kWh
$e_t^{BS,neg}$	Energy output when discharging the BS	kWh
$e_t^{BS,pos}$	Energy input when charging the BS	kWh
e_t^{DG}	Generated electricity of the DG	kWh
e_t^{DL}	Dump load	kWh
e_t^{PV}	Used electricity of the PV system	kWh
e_t^{PV+DL}	Total generated electricity of the PV system	kWh
e_t^{RO}	Consumed energy of the RO plant	kWh
$e_t^{RO,neg}$	Alteration rate of consumed energy of the RO plant	kWh
$e_t^{RO,pos}$	Alteration rate of consumed energy of the RO plant	kWh
g_t^{BS}	Auxiliary variable of the BS system for grid stability	kWh
s_t^{BS}	Storage level of the BS system	kWh
s_t^{WS}	Storage level of the WS	m³
$capacity^{BS}$	Number of BS units	Unit
$capacity^{PV}$	Installed kW_P of PV power	kW_P
w_t^{RO}	Outgoing water flux of the RO plant	m³

1 Introduction

The majority of experts in science, politics and nowadays even in economy, agree that the emissions of greenhouse gases need to be reduced in future. That is why renewable energy generation will increasingly be playing in order to satisfy the energy demand and to realize a reduction of greenhouse gas emissions. Due to the fluctuating nature of renewable energies, the entire power supply system faces new challenges to realize a stable and reliable supply and to reach a high penetration of renewable energies. Thus, new approaches to the electricity system are needed. One approach to increase the penetration of renewable energies is the utilization of flexible loads and energy storages. Energy management including the supply side, potential electricity storage as well as the demand side can help to balance production and consumption and to overcome the challenges of the intermittent character of renewable energy production (Mohammed, Mustafa, & Bashir, 2014).

In this thesis, the economic and functional interaction of flexible loads and photovoltaics (PV) power generation is analyzed in the context of isolated grids. Currently isolated areas, like islands or remote villages mostly rely on diesel generators for their energy supply. Grid connection or grid extension is often not possible due to high infrastructure investment (Fathima & Palanisamy, 2015; Hazelton, Bruce, & MacGill, 2014). Hence, decentralized diesel generators are the only possible way to ensure a reliable energy supply. This leads to a high dependency on the global oil price and on expensive diesel fuel in general. Therefore, renewable energy generation such as solar power plays an increasing role when it comes to isolated power supply considerations (Mofor, Isaka, Wade, & Soakai, 2013). Not only from an environmental, but also from an economical point of view, solar power and wind power are nowadays preferable to diesel generators. Thus, an increasing number of scientific publications deal with integrated renewable energy systems in isolated grids. The most common combination in implementation and research is a thermal power plant (diesel generator) with wind power, solar power or both. Several hybrid grids are already realized or in progress (Neves, Silva, & Connors, 2014). A study of 155 isolated grids revealed that the majority is found in regions with a very high solar irradiation (Werner & Breyer, 2012). Because of comparably higher prices for small wind turbines and a decrease of PV module prices in recent years, solar power has become the least costly choice for several isolated areas (Hazelton et al., 2014). Furthermore, the forecast of solar power is very reliable which makes it simpler to implement in existing grid structures. Remote areas often lack the understanding and required data of their wind regimes. Additional requirements for the construction and transport of a wind turbine leads to bigger effort and the need of a better infrastructure, often exceeding the resources of isolated communities (Mofor et al., 2013).

In order to further analyze the economic and functional interaction of flexible loads and PV power generation, a mathematical optimization model for an isolated grid and its system components based on economic issues is developed in this thesis. The main questions for this research are:

- How does the integration of a PV system influence the energy supply system and what is the capacity of the economically most beneficial PV system?
- How do flexible loads influence the utilization of the PV system and the optimal PV size capacity?
- How can a decentralized integration of flexible loads be implemented and what is the impact on the overall energy supply system?
- What are the most important uncertain input or system parameters and how do changes influence the model and its results?

In order to answer these questions, the thesis is structured as following: in chapter 2, the theoretical and technical background of the above mentioned research questions is presented. Chapter 3 is introducing the methodology for the optimization and the model itself. A case study using the developed model is presented in chapter 4. The results of the developed model are discussed in chapter 5. A conclusion and an overview for future research are given in chapter 6.

2 Background

2.1 Demand side management

Demand side management (DSM) is the ability to influence the electricity consumption of end users. It is seen as a possible way to reduce peak demand and to utilize the flexibility of the demand side which makes it possible to increase the penetration of renewable energies (Gelazanskas & Gamage, 2014). One example is to encourage end-users to reduce their loads during peak-times. Generally, DSM can be divided into four strategies:

- peak shaving: reduce demand at peak hours
- valley filling: increase load during off peak-times
- conservation: reduce entire energy demand of end-users
- load shifting: utilize flexible loads or energy storages to reschedule energy demand

The last mentioned strategy, load shifting seems as one of the most promising strategies, because it can meet the requirements of the demand and supply side in form of fluctuating renewable energy sources. By the utilization of flexible loads and storages, it should be guaranteed that a process is operated continuously with its required constraints (Lund, Lindgren, Mikkola, & Salpakari, 2015).

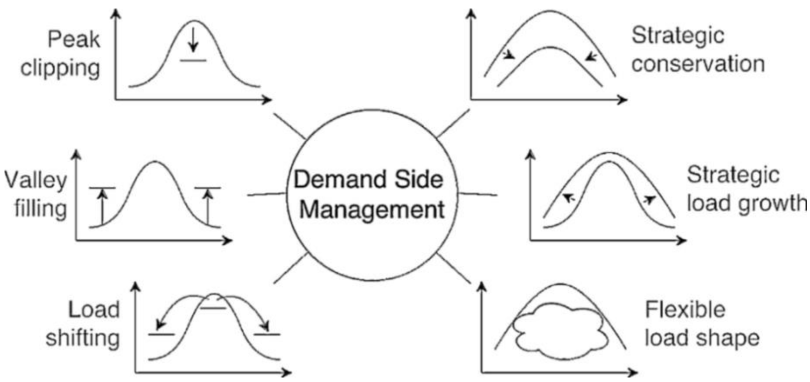

Fig. 1 Demand side management strategies (Gellings, 1985)

The technology which is used to realize demand side management is nowadays seen to be based on information communication technology (ICT) and advanced metering. Although ICT is an already long existing and mature technology, a widespread implementation of DSM has not been accomplished. Reasons are the lack of the required ICT infrastructure and the associated capital costs, the lack of standards and protocols for information transfer and in addition the lack of a developed market framework in which all players are integrated. Furthermore, security and safety risks and questions concerning the sensitive user data still have to be solved (O′Connell, Pinson, Madsen, & O′Malley, 2014). For isolated grids, DSM can play a major role to balance demand and the fluctuating power generation of renewable energies. The effect of DSM, like energy efficiency programs and flexible loads, on the energy system of the island Flores (Azores, Portugal) has been studied for a time horizon of ten years (Pina, Silva, & Ferrão, 2012). The authors conclude that the implementation of DSM strategies, especially load shifting, leads to a higher capacity factor of renewable energies and hence increases the profitability of renewable energy investments[1]. They observe that the application of load shifting saturates around 40% of the maximal possible load shifting potential. Another study examining the energy system of Flores in which the authors introduce different amounts of manageable demand, comes to similar results (Livengood, Sim-Sim, Ioakimidis, & Larson, 2010). The authors summarize that controllable demand helps to displace diesel-generated electricity and to increase the capacity factor of the existing wind and hydro power plants. They also observe that with higher rates of responsive demand the displacement of diesel-generated electricity declines, because load shifting is limited to one day. This effect is reduced when the possibility of load shifting into the next day is given.

2.1.1 Demand response

The distinction between DSM and demand response is not consistent. In this research, demand response is seen as one of the possible mechanisms to achieve demand side management, especially load shifting. As presented in Fig. 2, it is distinguished between incentive and time-based programs (Shariatzadeh, Mandal, & Srivastava, 2015). Incentive programs, for example direct load control, reward end-users when they provide flexible loads which can be controlled by a central control entity. In time-based programs, end-users are encouraged to actively participate in the electricity market by rescheduling their demand. This corresponds to the load shifting scenario presented in chapter 2.1. When utilizing distributed power generation, users also have the possibility to act as a power generator or reduce their

[1] Capacity factor: Ratio of actual produced energy over potentially produced energy for a certain time period

load for the grid. The incentive to change the consumption can be provided by variable electricity prices. Examples for variable electricity prices are time-of-use rates (TOU), critical peak pricing (CPP) and real-time pricing (RTP).

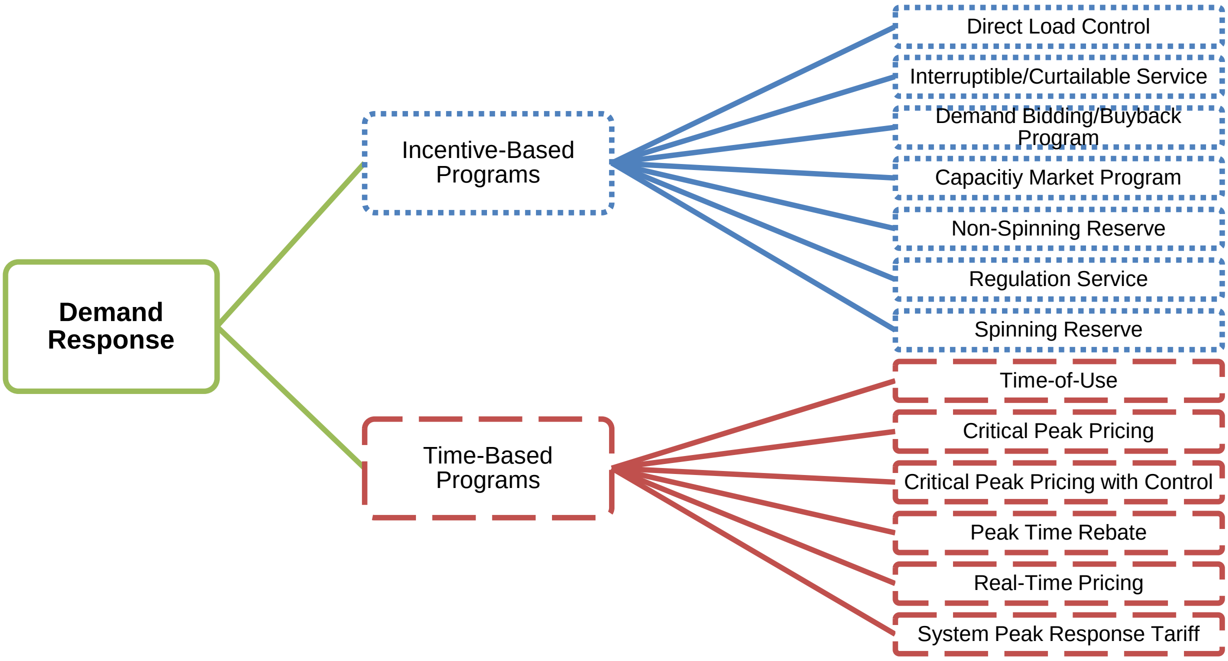

Fig. 2 Categorization of demand response programs

In TOU rates, electricity is more expensive during peak hours and cheaper during valley hours. This should lead to a reduced peak load and to an increase of load in valley hours. CPP is mostly offered to large industrial electricity consumers. It increases the electricity price during high peak-load events and thus consumers are expected to reduce their demand. RTP provides the end-user with a variable price for electricity and could for example represent the actual electricity production costs. The temporal resolution ranges from real time up to 1 hour and are hence often also called hourly prices (O'Connell et al., 2014; Shariatzadeh et al., 2015). Demand response can either be achieved by a central direct-controlled approach from system operator side or by a decentralized indirect-controlled approach in which the end-users themselves control their appliances (O'Connell et al., 2014). A comparison of these two different approaches with a high penetration of wind power in an isolated grid is conducted for the island Gran Canaria (Spain) (Dietrich, Latorre, Olmos, & Ramos, 2012). The centralized approach allows up to 30% of total costs savings on windy days with low demand and a capacity factor of 100% for the wind turbines is achieved. The decentralized approach does not reach as much savings in total costs, but it shows higher savings during peak hour periods. An implementation of demand response in an isolated grid is executed in King Island (Australia) (de Groot, Forbes, & Nikolic, 2013; Nikolic et al., 2014), the island Bornholm (Denmark) (Gantenbein, Binding, Jansen, Mishra, & Sundstrom, 2012) and Pulau Ubin Island (Singapore) (Fan, Rimali, Tang, & Nayar, 2012). For the island Sao Miguel (Azores), a RTP based demand response study with solar power production is conducted (Asensio & Contreras, 2014). The authors of this study observe a varying peak load with different solar power penetration. With moderate PV power integration, peak load decreases up to 6%. High PV power integration leads to an increase in peak load with up to 2.5% due to low price signals. Energy storage systems and demand response in an isolated grid with high shares of renewable energies have been also compared (Alharbi & Bhattacharya, 2013). Demand response results in lower total system cost and is therefore economically preferable to an energy storage system.

2.1.2 Decentralized smart grid control via electrical frequency

The grid frequency can serve as a universal measurement of the relation between electricity supply and demand. It decreases when supply exceeds demand and increases when demand exceeds supply. This feature is nowadays already used in traditional grid control and power generation scheduling. In future, end-users could be responsible of grid control by adjusting their demand according to the frequency. First investigations of how to use the frequency for demand response have been done more than 30 years ago (F.C. Schweppe, 1982). The same authors conclude that for a decentralized approach, the RTP time resolution should not be higher than five minutes. Beyond this resolution, a central grid control is needed to ensure grid stability (Fred C Schweppe, Caramanis, Tabors, & Bohn, 1988). Furthermore, a small time resolution reveals the actual costs of electricity production to end-users and maximizes economic efficiency. Another study of demand response controlled by frequency concludes that it definitely has the ability to stabilize the power network (Short, Infield, & Freris, 2007). A recent idea is to use the frequency to communicate real-time prices (Schäfer, Matthiae, Timme, & Witthaut, 2015). The price for electricity could be directly derived from the frequency. The authors of this study conclude that this approach leads to grid stabilization and to market equilibrium when short delay times in processing the frequency into the price signal are assumed. Further, it can be found in literature that decentralized demand response driven by price signals reduces peak demand (Barbato, Capone, Chen, Martignon, & Paris, 2015; Ramchurn, Vytelingum, Rogers, & Jennings, 2011). It is to notice that multiple studies also observe new peaks caused by low price signal response (Gelazanskas & Gamage, 2014). A case study with two large industrial consumers in Ireland shows that price signals lead to a higher utilization rate of wind power (Finn & Fitzpatrick, 2014). The influence of decentralized demand response in isolated grids has also been studied (Ramos, Canizares, & Bhattacharya, 2014). The authors state that demand response can be added to the total demand not only once, since smart devices and also users learn from the past and therefore adapt their future behavior, resulting in a two-way dependency of demand and price and a kind of iterative demand adjustment. A decentralized demand response system based on frequency as price signal would require much less hardware and investment costs compared to the "traditional" ICT approach. Additionally privacy and security issues do not occur. This idea is pursued by the start-up *Easy Smart Grid GmbH* from Karlsruhe (Walter, 2014).

2.2 Flexible loads

As earlier discussed in this thesis, flexible loads are essential for any demand response program, because only they can enable a rescheduling of the load profile and hence a load shifting. Flexible loads can be distinguished between households, service sector and industrial loads. Household loads can be further divided into shiftable static loads and thermal loads (Ramchurn et al., 2011). Examples for shiftable static loads are devices like washing machine and dishwasher. These devices show a precise running time and load pattern. Thermal loads, like freezer, refrigerator, water heating and space heating depend on the usage and the ambient temperature. Flexible loads in the service sector are of the same kind as in households. Examples are ventilation systems, hot water generation, food store refrigerators, air conditioning, night storage heaters and municipal waste water treatment (Lund et al., 2015). Desalination systems can also be classified to the service sector loads. Reverse osmosis (RO) desalination is used for the further investigation on flexible loads in this paper. Industrial loads are often seen as an electrical base load, but some industrial processes are also already under control of the system operator and hence are handled as flexible loads. Electricity storage systems, like batteries represent a different kind of flexible loads and have to be regarded separately.

2.2.1 Desalination as flexible load

Desalination capacities are increasing worldwide as drinking water is becoming a more and more rare resource, especially in coastal-like and desert-like areas. In these regions mostly abundant renewable energy resources are available. As desalination is a potentially flexible and energy intensive process, it seems very attractive to combine it with renewable energy sources (Tzen & Papapetrou, 2012). Desalination processes can be classified into thermal and electrical processes (Mathioulakis, Belessiotis, & Delyannis, 2007). First, thermal desalination processes comprise multi-stage flash, multi-effect, vapor compression and humidification-dehumidification desalination. Second, electrical processes are actually mechanically driven membrane processes and are represented by mechanical vapor compression and RO desalination. RO is seen as the technology of choice as it has a much lower specific energy consumption per produced m^3 of water (2-6 kWh/m^3 for membrane processes compared to 7-14 kWh/m^3 for thermal processes) (Subramani, Badruzzaman, Oppenheimer, & Jacangelo, 2011). Furthermore, 31% of the current desalination plants which are utilizing renewable energy sources are based on RO technology and solar power (Papapetrou, Wieghaus, & Biercamp, 2010). The desalination process in this thesis should be regarded as a flexible load in the electrical grid. Hence, RO is the technology that is investigated. RO achieves desalination by a semi-permeable membrane. The salty feedstock is pressed through the membrane by pumps. Salt is retained at the feedstock side while water passes through. The pressure which has to be applied has to be higher than the osmotic pressure. Nowadays, RO is applied as a constant process. But several studies already investigated the variable operation of this technology. A concept for a variable RO plant driven by wind energy is presented by *ENERCON GmbH* (Paulsen & Hensel, 2007). Their system consists of four modular RO units, each continuously adjustable from 50% to 100% of its power rating. The *ENERCON* system has a variable water production output from 12.5% to 100% of its rated capacity and a specific energy consumption of 2.0 kWh/m^3 to 2.5 kWh/m^3. In a case study on the island Utsira in Norway, it has been observed that 100% of the annual energy demand can be supplied by wind energy due to the flexible operation. The investigation of different operational strategies for a RO plant is modeled (Pohl, Kaltschmitt, & Holländer, 2009). The authors investigate four operational strategies (energy consumption, load range, pressure alteration and permeate quality) for a wind power driven optimal variable operation. A broad load range with low specific energy consumption is realized with a constant recovery strategy which allows an operation of the desalination unit even under low energy supply. A RO system of one unit with a RO system made up of three units is compared (Peñate, Castellano, Bello, & García-Rodríguez, 2011). Both systems are powered by wind energy and a case study for Gran Canaria is conducted. Another modular and variable RO plant which can be driven by renewable energies is presented by *SYNLIFT Systems GmbH* (Käufler, Pohl, & Sader, 2012). It consists of two RO units. Both can be shut down and operated continuously between 50% and 150% of their rated power. Furthermore, it is investigated if variable operation leads to a decrease in performance and efficiency due to membrane damages. They conclude that variable operation is totally feasible.

2.2.2 Battery storage

Battery storage (BS) systems are one kind of several energy storage systems, which are distinguished between electrical, mechanical, chemical and thermal energy storage technologies (Akinyele & Rayudu, 2014). To start with, electrical energy storage systems are, for example, supercapacitors and superconducting magnetic energy storage. Further pumped hydro storage, compressed air storage and flywheels belong to mechanical energy storages. Batteries and hydrogen storage systems are chemical storage technologies. Last, energy storage systems can be characterized by their energy storage capacity (kWh), energy density (Wh/l), power density (W/l), charge/discharge duration, power output (kW), response time, lifetime (years or cycles), round-trip efficiency and capital cost ($/kW or $/kWh) (Castillo & Gayme, 2014).[2] Energy storage can have several positive benefits for the whole system: grid stabilization, power quality management, load shifting and grid operational supports (Mohammed et al., 2014). Although in general energy storage is a net consumers in the grid due to the conversion losses, it is seen as the technology

[2] Round-trip efficiency: the ratio of energy used for charging to the resulting discharged energy

which can possibly overcome the issues of fluctuating renewable energy production and which can increase the energy and economic efficiency of the electricity system (Lund et al., 2015). These benefits can be even higher for isolated grids, as electricity supply is in general more expensive and voltage constraints are higher due to the small size (Rious & Perez, 2014). Pumped hydro storage is seen as the most mature and advanced storage technology. Its utilization would require hydroelectric dams and large water reservoirs. Therefore, this technology cannot be considered in the case of isolated grids and especially islands. The same applies to compressed air storage. Electrical energy storage systems are short term storages and therefore not further considered in this thesis. BS systems are already widely applied in isolated grids and fit their needs the best, because they are seen as the most flexible, reliable and responsive technology (Chauhan & Saini, 2014; Rious & Perez, 2014). Batteries store energy in form of electrochemical compounds in cells. The desired voltage and capacity is achieved by connecting cells in series or parallel (Fathima & Palanisamy, 2015). There are various types of batteries with different properties, advantages and disadvantages.

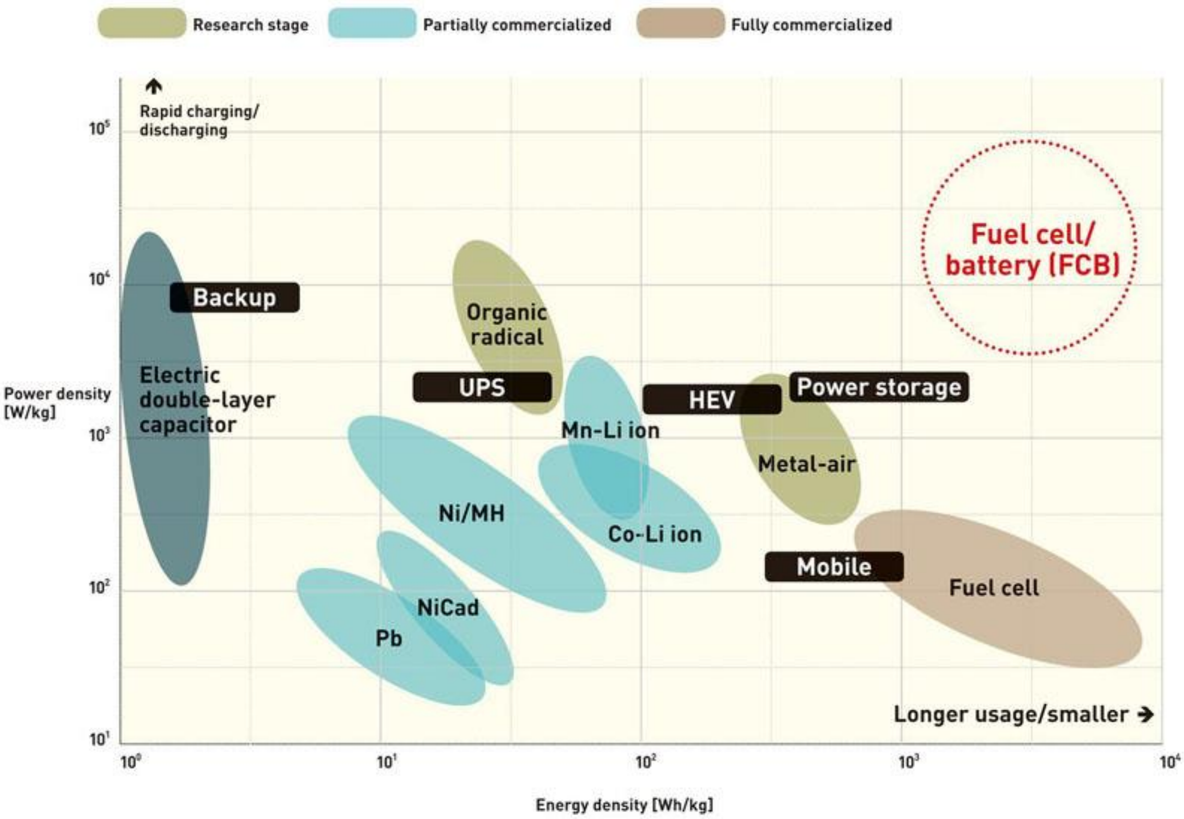

Fig. 3 Ragone plot for several batteries comparing their performance (Tsutsumi, 2012)

Fig. 3 gives an overview of the performance of different chemical energy storage technologies. Common drawbacks of batteries are self-discharge and a decreasing performance with increasing cycles. Operation and maintenance cost of batteries are low, compared to the capital and replacement costs which represent the main costs (Lund et al., 2015). The most popular and mature battery technologies are lead-acid, nickel-cadmium, sodium-sulfur and lithium-ion batteries. Lead-acid batteries have already been widely used for decades. Their major advantages are the comparably low cost per kWh of energy capacity and their maturity. Disadvantages are their low life cycle (500-1000 cycles), low energy density (30-50 Wh/kg), failure of deep discharge and the associated environmental impacts. The batteries round-trip efficiency is around 70-90%. Nickel-cadmium batteries have similar environmental issues. Compared to lead-acid batteries, nickel-cadmium batteries show better technical properties, including a much higher energy density (50-75 Wh/kg) and higher robustness in operation and temperature. They have a medium short life cycle (2000-2500 cycles), and are relatively more expensive. Sodium-sulfur batteries are high temperature batteries and hence are operating at 300-350°C. Heat energy from own-stored energy is used to reach this temperature. They are characterized by no self-discharge, a round-trip efficiency of 90% and a high energy density. Additionally, larger installations are preferable. Like lead-acid batteries, lithium-ion batteries are already widely implemented. They show a high energy density (75-200 kWh/kg), high life cycle (around 10000 cycles), low self-discharging and a high round trip efficiency. Furthermore, no memory effect is observable. The drawback of the lithium-ion technology is its high costs for large installations (Akinyele & Rayudu, 2014; Chauhan & Saini, 2014; Lund et al., 2015; Mahlia, Saktisahdan, Jannifar, Hasan, & Matseelar, 2014; Yekini Suberu, Wazir Mustafa, & Bashir, 2014). It is expected that further research will lead to advances in already existing battery technology, resulting in lower costs, higher efficiencies and higher energy densities, and to new battery technologies, like flow batteries which are currently just emerging (Rious & Perez, 2014).

2.3 Isolated grid

All reviewed studies on the sizing and controlling of hybrid grid components in an isolated grid deal with at least one renewable energy source, an energy storage system and a traditional power generation unit, mostly powered by diesel fuel. Most of the studies include solar power and wind power possibilities. Different storage systems are regarded, ranging from one to several battery technologies, pumped hydro storages, flywheels and hydrogen production combined with fuel cells. In the literature most often hourly steps are chosen for the temporal resolution. The optimization objective differs from a single economical objective, like the levelized cost of energy (LCOE) or the total net present cost, to multi objectives including also the loss of power supply or environmental aspects, like CO_2 emissions. For the optimization, commercial software like HOMER, H2RES or mathematic models solved by particle swarm optimization, iterative processes, differential evolution algorithms or mixed integer liner programming are utilized.

Table 1 Different modeling approaches of a hybrid grid with desalination

Author	Focus	Components	Desalination	Objective	Optimization approach	Case study
Setiawan, Zhao, and Nayar (2009)	Sizing; laboratory experiments on inverter and RO	Wind, PV, BS, DG	Operation deferrable (8h/d); water tank for two days	Minimization: Annualized capital cost, LCOE, net present cost	HOMER	Maldives
Raquel Segurado, Krajačić, Duić, and Alves (2011)	Sizing with horizon till 2030	Wind, DG, pumped hydro	Water tank for 5 days	Maximization: Renewable penetration	H2RES	Cape Verde
Kristina Bognar, Blechinger, and Behrendt (2012)	Sizing; different strategies for desalination	Wind, PV, BS, DG	Operation with excess energy, constant or deferrable; water tank for two days	Minimization: Total net present cost	HOMER	Grenada
K. Bognar, Pohl, and Behrendt (2013)	RO integration and modeling (variable pressure, power flow); sizing of battery	Wind, BS, DG	Operation constant, discontinuous	Minimization: LCOE	HOMER	Cape Verde
Novosel et al. (2014)	Energy management with 30% of traditional power	RO with pumped hydro, wind, PV	Water demand hourly constant; different desalination capacities	Maximization: Renewable penetration	EnergyPLAN	Jordan
R. Segurado, Costa, Duić, and Carvalho (2015)	Investment and operational optimization	Wind, PV, BS pumped hydro	Operation with wind excess energy	Minimization: Costs with highest penetration of wind	H2RES	Cape Verde

In general, many case studies are conducted to present the developed models. These range from island systems, to the electrification of rural villages or households. All studies reviewed for this thesis are listed in the Table 18 in the appendix. Several papers also include desalination units in their investigation of isolated hybrid energy systems. The consideration differs from the unit sizing of desalination plants and the optimal operational strategy in a hybrid system. They investigate RO as desalination technology and use commercial software (HOMER, H2RES, EnergyPlan). They also either include batteries or pumped hydro storages as can be seen in Table 1.

2.3.1 PV power generation

Photovoltaics (PV) power generation utilizes directly the incoming solar irradiation from the sun by converting it into direct current. The photons hitting a solar cell induce a direct current in the cell. This current can be amplified and inverted to the desired alternate current. In practice, several cells are connected in series and parallel, and are called a solar module (Fathima & Palanisamy, 2015). Different technologies have been developed which can be classified in mono-crystalline, poly-crystalline and thin-film cells. PV modules manufactured out of crystalline silicon are the most common and popular technology. As an indirect semiconductor, they reach a theoretical efficiency of 30%. Nowadays multi-crystalline cells reach an efficiency of 16%, while mono-crystalline cells reach 17 to 20%. As silicon has a relative low absorption coefficient, these solar cells need to be built comparably thick. Thin-film cells can be built with very little material and thus could provide a high cost reduction potential. Examples of thin-film cells are amorphous silicon, cadmium-telluride, copper-indium-selenium and organic solar cells. Commercially available thin-film solar cells do not reach the same high efficiencies yet, but with further research this is expected to change in the future. Fig. 16 in the appendix shows the efficiency records for different PV technologies in research for the last 40 years. (Kristina Bognar, 2013; Journeay-Kaler & Mofor, 2013)

2.3.2 Diesel generator

Diesel generators (DG) are the most common way to meet electricity demand in isolated areas. Also in future hybrid grid systems, they will be needed as reliable power source or as backup system (Bajpai & Dash, 2012). A characterization of a diesel generator is done by its efficiency, its hourly fuel consumption and its specific fuel consumption (Yamegueu, Azoumah, Py, & Zongo, 2011). The efficiency is the highest in the operation window of 80-100% of its rated power. The minimal load of a diesel generator should be not less than 25% of the rated power as efficiency decreases and wear and tear increases (Schies, 2013). This effect can be seen in Fig. 4. The rated power is commonly chosen as the expected peak load. The operation strategy can either be load following or constant power delivery. This will lead to party-load operation of the diesel generator in a load following operation strategy and hence it will not run in its technical optimum. As a consequence, it could be advantageous to operate two diesel generators with half capacity. (Journeay-Kaler & Mofor, 2013)

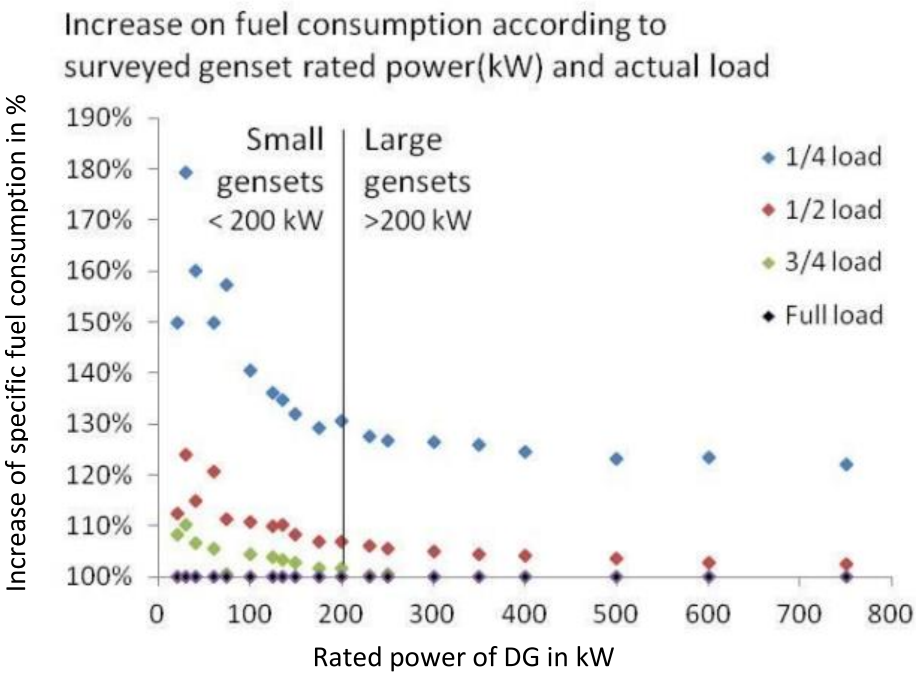

Fig. 4 Efficiency of DG for different load factors (Schies, 2013)

2.3.3 Grid configuration and grid control

With the integration of highly fluctuating renewable energies, new challenges for the regulation of voltage and frequency in electricity grids arise. These challenges are even higher in smaller grids, due to their volatile load profile. Therefore, an energy management with suitable control strategies has to be developed (Journeay-Kaler & Mofor, 2013). This should provide primarily grid stability by balancing demand and supply, but also optimize the interaction of all components. It can be differentiated by the unit which is responsible for balancing demand and supply. Three types of configurations for the integration of PV power in microgrids can be formed and are displayed in Fig. 5 (L. A. C. Lopes, Katiraei, Mauch, Vandenbergh, & Arribas, 2012):

- multi-master DG dominated grid architecture
- single switching master grid architecture
- multi-master inverter dominated grid architecture

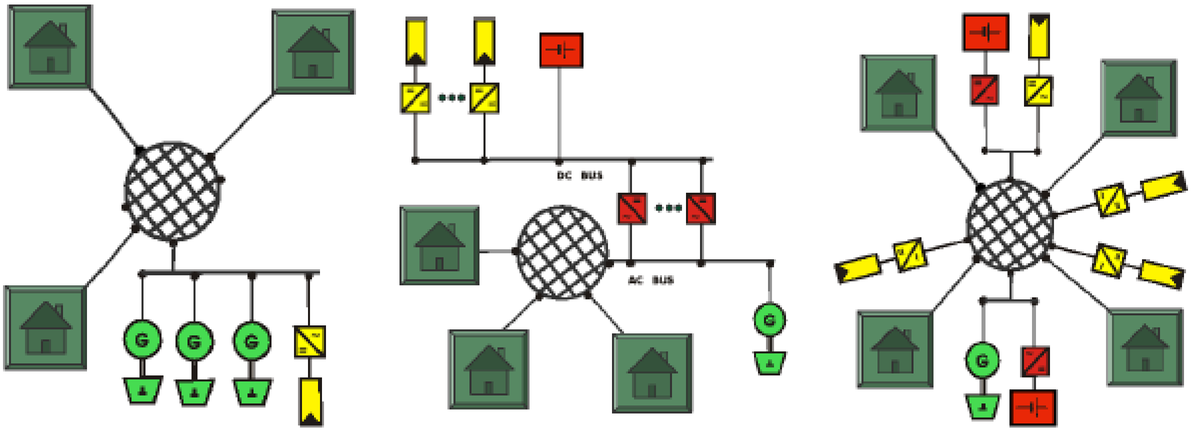

Fig. 5 Schemes of isolated grid configurations with PV integration (L. A. C. Lopes et al., 2012)

In a multi-master DG dominated grid, the responsibility for the desired power quality and system stability has one or several DGs. At least one of the DGs has to run continuously to guarantee this function. PV power can be easily integrated in the grid with direct current (DC) to alternate current (AC) inverters. However, it must be assured that the DG is not running below its minimal loading factor (reasons are stated in chapter 2.3.2). This restricts the maximal renewable penetration in the grid.[3] To increase the renewable penetration, excess power of renewables can be curtailed. A commercial implementation to curtail PV power is, for example, already offered by *SMA Solar Technology AG* with their SMA FUEL SAVE CONTROLLER ("SMA FUEL SAVE CONTROLLER"). The complete shutdown of the DG is only possible with adequate energy storage capacity, resulting in the single switching master grid architecture. The controlling responsibility is switched between DG and the AC-DC inverter of the PV and battery unit, allowing the DG to shut down. This requires additional communication between the system units and a master unit to realize an appropriate energy management and switch between the different

[3] Instantaneous renewable penetration: Ratio of the power drawn by renewables and the total load

operating modes. Such a configuration is suitable for smaller grids like isolated villages. The multi-master inverter dominated grid is designed for larger grids with additionally distributed AC sources like distributed PV or DG power stations. The stability of the grid is guaranteed by certain DGs and several, varying inverters. In this case, a specific communication is not required, because the electrical properties of voltage and frequency, like in conventional power systems, are used for stabilizing the grid. Other ideas of configurations for the integration of PV power can be also found in the following literature: Arul, Ramachandaramurthy, and Rajkumar (2015); Carmeli, Castelli-Dezza, Mauri, Marchegiani, and Rosati (2012); Chauhan and Saini (2014); Nehrir et al. (2011); Nema, Nema, and Rangnekar (2009); S. Upadhyay and Sharma (2014).

3 Mathematical optimization approach

An overview of different optimization approaches for hybrid grids is given in chapter 2.3. In this thesis, a mathematical model with several sub-models is developed and implemented in the *General Algebraic Modeling System* (GAMS). The program code can be found in the appendix. Each sub-model is presented in chapter 3.2. The optimization model is formulated as a linear program (lp) or mixed integer linear program (milp), depending on if an on/off operation for the diesel generator and desalination system is desired. To solve the lp/milp, the integrated Cplex solver from IBM is selected. With the required deterministic input data for one representative year (PV supply per kW peak, electricity demand, water demand), the decision variables, like the optimal investment for the PV power station and the BS, as well as the operation and energy management strategy, are determined by minimizing the equivalent annual total costs.

3.1 Optimization of LP/MILP using GAMS and Cplex

The mathematical model is implemented in the software GAMS. GAMS is an algebraic programming language which enables the user to formulate and solve large complex mathematical models. It has been originally developed by the World Bank in the 1970´s (Bussieck & Meeraus, 2004). GAMS does not solve the problem itself. Instead it calls third party solvers, like Cplex, Gurobi or ZIMPL (Chattopadhyay, 1999). Nowadays, the used solver Cplex contains a variety of algorithms, but is named after the simplex method implemented in the programming language C. The mathematical model is formulated intentionally as lp or milp. In lp all equations, including the objective function, contain decision variables with linear relationships. A lp problem can be represented by a convex geometric polytope, which is shaped by the constraint equations of the problem. The geometric idea to maximize/minimize the objective function is to search along the edges of the polytope for the solution with the highest objective function value, because an optimal solution is always located on the shell of the polytope due to its convex shape. Therefore, the algorithm "walks" from an edge with a possible solution to the edge with a higher value for the objective function. When considering an off/on behavior, for example for the desalination unit or the diesel generators, the model has to be formulated as a milp by introducing binary variables. For mixed integer programming the Cplex solver utilizes several methods, like branch-and-bound, branch-and-cut, branch-and-price and the cutting-plane method. In general, the milp is solved with a relaxation of the integer condition as a lp. This provides a first solution, which is not valid, but which is used as a lower bound. The actual milp is branched with different integer assumptions and solved subsequently. The branch with the lowest gap to the lp solution forms the upper bound and is further investigated. The integer assumptions result in a decision tree of the problem which can be "cut" down due to the bounds and heuristic methods. The optimal integer solution is obtained, when the difference to the optimal bound solution is lower than a predefined gap tolerance.

3.2 Mathematical model

The model for the optimization of the isolated grid consists of sub-models, which are presented in the chapters 3.2.1 to 3.2.7. The sub-models and their interrelation are shown in Fig. 6. The red continuous arrows symbolize the electricity flow while the blue dashed arrows are the water flow.

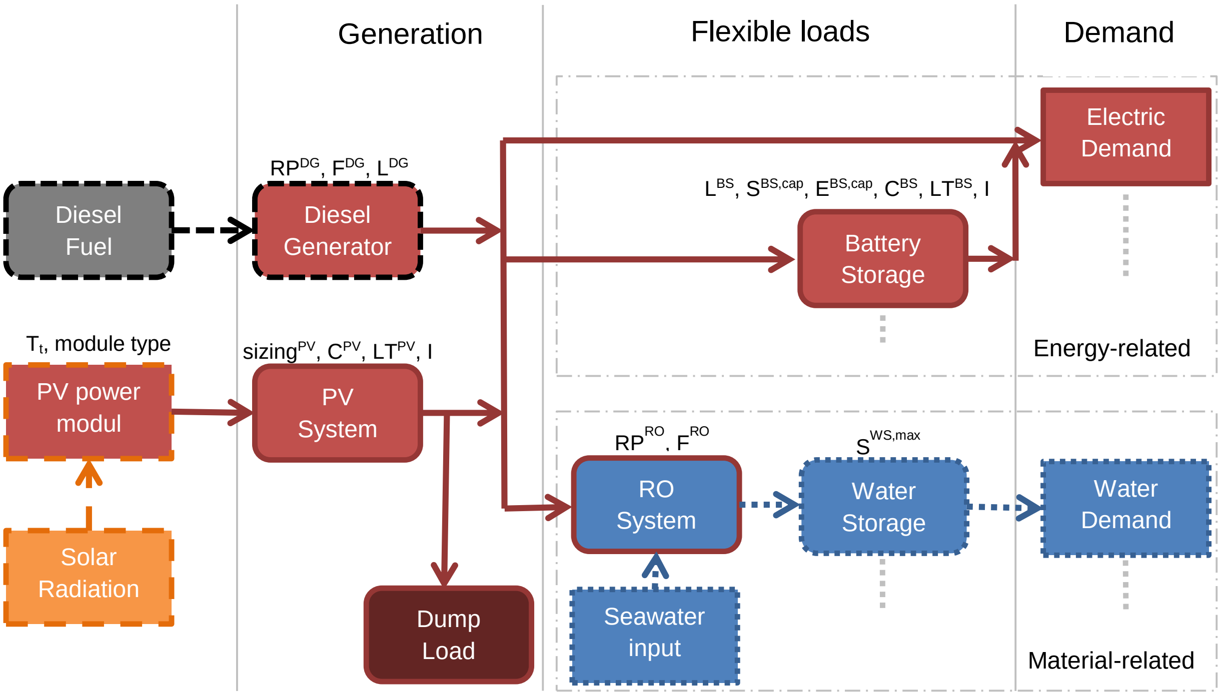

Fig. 6 Scheme of the isolated grid, with PV power generation and flexible loads

The system components are visualized with different shapes, depending on their nature. Input data, like the electric demand, the water demand and the solar radiation are displayed with an angular shape. The rounded rectangles, like the DG, the PV system and the RO system, are components which are changed during the optimization process and depend on decision variables. The corresponding input system parameters are listed above the items. The flexible loads, storages and demands can be also composed of different kinds like implied in Fig.6. For the energy part, the most popular example are heating and cooling loads. Examples for the material part are industrial processes like paper production, ice production etc.. The time steps are displayed with the indices t and a temporal resolution of 15 min per time step is selected. Thus, 35040 time steps for one year are taken into consideration. In the following equations, variables are expressed with small letters, while parameters are expressed with capital letters.

3.2.1 Objective function and main constraints

The objective of the optimization is to minimize the equivalent annual total costs. This is represented by the following equation in which the costs are determined by the costs of the DG, the PV system and the BS:

$$\min_{\{\mathrm{Decision\ Variables}\}} \mathrm{cost}^{\mathrm{total}} = \tag{3.1}$$

$$\mathrm{cost}^{\mathrm{DG}}(\mathrm{diesel}_{\mathrm{t}}^{\mathrm{DG}}) + \mathrm{cost}^{\mathrm{PV}}(\mathrm{capacity}^{\mathrm{PV}}) + \mathrm{cost}^{\mathrm{BS}}(\mathrm{capacity}^{\mathrm{BS}})$$

The decision variables are the rated peak power of the PV system ($\mathrm{capacity}^{\mathrm{PV}}$), the installed unit size of the BS ($\mathrm{capacity}^{\mathrm{BS}}$) and the diesel used by the DG in each time step ($\mathrm{diesel}_{\mathrm{t}}^{\mathrm{DG}}$). When minimizing the objective function, the model has to fulfil certain constraints. The main constraints are the satisfaction of the electricity demand ($\mathrm{E}_{\mathrm{t}}^{\mathrm{Demand}}$) and the water demand ($\mathrm{W}_{\mathrm{t}}^{\mathrm{Demand}}$) in each time step. The electricity demand and the required energy for the RO plant ($\mathrm{e}_{\mathrm{t}}^{\mathrm{RO}}$) have to be supplied by the DG ($\mathrm{e}_{\mathrm{t}}^{\mathrm{DG}}$), the PV system ($\mathrm{e}_{\mathrm{t}}^{\mathrm{PV}}$) or by discharging the BS ($-\mathrm{e}_{\mathrm{t}}^{\mathrm{SB}}$). Excess energy can be used for charging the battery ($\mathrm{e}_{\mathrm{t}}^{\mathrm{SB}}$). This results in the following balancing equation for the electricity flux:

$$\mathrm{E}_{\mathrm{t}}^{\mathrm{demand}} + \mathrm{e}_{\mathrm{t}}^{\mathrm{RO}} + \mathrm{e}_{\mathrm{t}}^{\mathrm{BS}}(\mathrm{capacity}^{\mathrm{BS}}) = \mathrm{e}_{\mathrm{t}}^{\mathrm{DG}} + \mathrm{e}_{\mathrm{t}}^{\mathrm{PV}}(\mathrm{capacity}^{\mathrm{PV}}, \mathrm{e}_{\mathrm{t}}^{\mathrm{DL}}) \qquad \forall \mathrm{t} \tag{3.2}$$

All terms are expressed in kWh. All variables, except for the electricity flow of the battery are of exclusive positive type (x≥0). e_t^{SB} can be either positive when charging, or negative when discharging.

The water demand (W_t^{Demand}) has to be supplied by the water storage (WS). The storage level is expressed by s_t^{WS}. The current level is derived by the previous level (s_{t-1}^{WS}), the incoming water flux from the RO plant (w_t^{RO}) and the outgoing water demand:

$$s_t^{WS} + W_t^{demand} = s_{t-1}^{WS} + w_t^{RO} \qquad \forall t \tag{3.3}$$

The last storage level (t=35040) is thereby the initial level for the first value to achieve a yearly circular behavior.

3.2.2 PV system

The energy generated by the PV system depends mainly on the incoming solar irradiation and the capacity of the installed PV system. The given data of the irradiation are utilized by an already developed PV program of the IIP. This program considers a specific module type, temperature, orientation of the modules, several losses and indirect and direct radiation. It can be calculated how much energy is generated by a system with an installed capacity of 1 kW_P ($E_t^{PV1kW_P}$). The generated energy is obtained by multiplying the installed peak power for the optimal PV system ($capacity^{PV}$ in kW). Thus, this is a decision variable and a result of the optimization process. It is divided by the factor four to convert the hourly produced energy to 15 min steps. When PV power generation is exceeding the demand, it can be curtailed by a dump load (e_t^{DL}):

$$e_t^{PV} = E_t^{PV1kW_P} \cdot {capacity^{PV}}/{4} - e_t^{DL} \qquad \forall t \tag{3.4}$$

The resulting annual cost of the PV system is expressed as an annuity and determined by the installed peak power, the price per peak power (C^{PV} in $/ kW_P) and the annuity factor (A^{PV}):

$$cost^{PV} = C^{PV} \cdot A^{PV} \cdot capacity^{PV} \tag{3.5}$$

The annuity factor for the PV system is defined by the life time (LT^{PV} in years) and the interest factor (I):

$$A^{PV} = \frac{(1+I)^{LT^{PV}} \cdot I}{(1+I)^{LT^{PV}} - 1} \tag{3.6}$$

3.2.3 Diesel generator

The diesel-generated electricity is a decision variable and hence a result of the optimization. With the specific fuel consumption ($F^{DG,A}$) and the additional fuel consumption for the quarterly loaded DG (L^{DG}), it is possible to calculate the characteristic values $F^{DG,B}$ and $F^{DG,C}$ for the linear modelling approach for a DG with decreasing efficiency, like presented by Yamegueu et al. (2011):

$$F^{DG,C} = L^{DG} \cdot F^{DG,A}/3 \qquad \forall t \tag{3.7}$$

$$F^{DG,B} = F^{DG,A} - F^{DG,C} \qquad \forall t \tag{3.8}$$

The consumed diesel fuel is calculated with the characteristic values for the DG and the produced electricity of the DG:

$$diesel_t = e_t^{DG} \cdot F^{DG,B} + {RP^{DG}}/{4} \cdot F^{DG,C} \qquad \forall t \tag{3.9a}$$

The generated electricity is limited in both cases by the rated power of the DG:

$$e_t^{DG} \leq {RP^{DG}}/{4} \qquad \forall t \tag{3.10a}$$

For these linear approaches, the constraint for the minimal loading is developed in chapter 3.2.5 as it is related to questions of the grid stability. The drawback of these approaches are that diesel consumption is assumed even when the DG is in idle-mode and no electricity is produced. Therefore, a binary variable (b_t^{DG}) can be introduced to switch off the DG completely:

$$diesel_t = e_t^{DG} \cdot F^{DG,B} + F^{DG,C} \cdot b_t^{DG} \cdot {RP^{DG}}/{4} \qquad \forall t \tag{3.9b}$$

Additional constraints assure that the DG is switched on and off accordingly and that low loading is avoided:

$$e_t^{DG} \leq b_t^{DG} \cdot RP^{DG}/_4 \qquad \forall t \tag{3.10b}$$

$$e_t^{DG} \geq b_t^{DG} \cdot RP^{DG}/_{16} \qquad \forall t \tag{3.11}$$

The cost of the DG is calculated by its consumed fuel and its price (C^{diesel} in \$/l):

$$cost^{DG} = \sum diesel_t \cdot C^{diesel} \tag{3.12}$$

Further capital costs for the DG are not considered, as already existing DG for the power supply are assumed.

3.2.4 Battery storage

The state of charge for the BS for a time step depends mainly on the state of charge of the previous time step and the charging or discharging of the battery for this time step. Like for the WS, the storage level of the first time step (t=1) depends on the storage level of the last time step (t=35040). Additionally, the round-trip-efficiency ($L^{BS,rte}$) and self-discharging losses ($L^{BS,sdl}$) have to be considered:

$$s_t^{BS} = s_{t-1}^{BS} \cdot \left(1 - L^{BS,sdl}\right) + e_t^{BS} - e_t^{BS,neg} \cdot (1 - L^{BS,rte}) \qquad \forall t \tag{3.13}$$

The charging and discharging losses are derived from the negative part of e_t^{BS}, which is determined by:

$$e_t^{BS} = e_t^{BS,pos} - e_t^{BS,neg} \qquad \forall t \tag{3.14}$$

Where $e_t^{BS,pos}$ represents the charging flux and $e_t^{BS,neg}$ the discharging flux. Both auxiliary variables are strictly positive. The stored energy has to be lower than the capacity of the resulting BS system, which is described by the amount of battery units ($capacity^{BS}$) and the energy capacity per battery unit ($S^{BS,cap}$ in kWh/unit):

$$s_t^{BS} \leq capacity^{BS} \cdot S^{BS,cap} \qquad \forall t \tag{3.15}$$

Accordingly, the electricity flux e_t^{BS} is limited by the power capacity of the given battery ($E^{BS,cap}$ in kW/unit):

$$e_t^{BS} \leq capacity^{BS} \cdot E^{BS,cap}/_4 \qquad \forall t \tag{3.16}$$

$$e_t^{BS} \geq -\text{capacity}^{BS} \cdot E^{BS,cap}/_4 \qquad \forall t \tag{3.17}$$

The annual cost for the BS is again modeled as annuity and depends on the amount of the battery units, the price per battery unit (C^{BS} in $/unit) and the annuity factor of the battery:

$$\text{cost}^{BS} = C^{BS} \cdot A^{BS} \cdot \text{capacity}^{BS}/L^{BS,dd} \tag{3.18}$$

The annuity factor can be determined accordingly to equation 3.5:

$$A^{BS} = \frac{(1+I)^{TL^{BS}} \cdot I}{(1+I)^{TL^{BS}} - 1} \tag{3.19}$$

3.2.5 Grid stability

The grid stability has either be guaranteed by a running DG or by the BS. For the DG, it has to be assured that it is not loaded less than 25% of its rated power. The battery should at least provide half of the rated power of the DG when being responsible for grid stability. Therefore, the auxiliary variable g_t^{BS} is introduced in the following equation:

$$g_t^{BS}/_2 + e_t^{DG} \geq RP^{DG}/_4 \qquad \forall t \tag{3.20}$$

This variable has to meet further constraints. First, it has to guarantee that there is enough energy stored in the battery at every time step:

$$g_t^{BS} \leq s_t^{BS} \qquad \forall t \tag{3.21}$$

Second, it has to ensure that the battery can provide half as much power as the rated power of the DG:

$$g_t^{BS} \leq \text{capacity}^{BS} \cdot E^{BS,cap} \qquad \forall t \tag{3.22}$$

3.2.6 Desalination system

The RO plant is characterized by its energy consumed (e_t^{RO}) and its water output (w_t^{RO}). These entities are related to each other by the conversion factor of the RO system (F^{RO} in kWh/l). An infinitesimal loss factor (L^{RO}) multiplied with the alteration rate of the consumed energy, is also included:

$$e_t^{RO} + L^{RO} \cdot e_t^{RO,neg} = w_t^{RO} \cdot F^{RO} \qquad \forall t \tag{3.23}$$

In the reviewed papers, no characterizations of RO losses have been found. In this thesis, the loss factor is included to moderate the operation of the RO plant and to avoid a jumping on/off behavior:

$$e_t^{RO} - e_{t-1}^{RO} = e_t^{RO,pos} - e_t^{RO,neg} \qquad \forall t \tag{3.24}$$

All introduced variables for the desalination system are strictly positive. The consumed power of the RO unit is limited by its rated power (RP^{RO}) and as a consequence also the maximal water output is limited:

$$e_t^{RO} \leq {RP^{RO}}/{4} \qquad \forall t \tag{3.25a}$$

Furthermore, a milp model for the RO system is developed to restrict the minimal possible operating point to 25 % of the rated power by introducing the binary variable b_t^{RO}:

$$e_t^{RO} \leq {RP^{RO}}/{4} \cdot b_t^{RO} \qquad \forall t \tag{3.25b}$$

$$e_t^{RO} \geq {RP^{RO}}/{16} \cdot b_t^{RO} \qquad \forall t \tag{3.26}$$

The saltwater input is considered abundant and therefore without any constraints. Costs for the desalination system are not part of the optimization process. They are analyzed separately with the results of the optimization.

3.2.7 Water storage

The maximal storage capacity is set to be equivalent to the averaged water demand for a certain number of days ($S^{WS,max}$). This leads to the following constraint for the storage level for all time steps:

$$s_t^{WS} \leq \sum W_t^{demand} \cdot {S^{WS,max}}/{365} \qquad \forall t \tag{3.27}$$

No costs for the WS system are assumed.

3.3 Decentralized integration of a flexible load with a price signal

The decentralized integration approach of the flexible load is realized with a variable price signal for each time step. All introduced constraints of the previous chapters are still valid and essential. However, the objective of the optimization changes to the minimization of the arising costs for the desalination plant due to its consumed energy:

$$\min_{\{\text{Decision Variables}\}} \text{cost}^{\text{RO}} = \text{P}_{\text{t}}^{\text{RO}} \cdot \text{e}_{\text{t}}^{\text{RO}} \tag{3.28}$$

The decision variables only consist of the energy consumption of the RO system in each time step. For a better understanding of the decentral control, the price signal has to be further analyzed. The price signal is modeled as a parameter to realize again a linear programming problem. For a first understanding, it is assumed that the price signal represents the actual electricity production costs, which is a mix price based on the ratio of supplied DG electricity and PV electricity. The RO plant is a large consumer in the grid, and hence a very strong dependency between the price for electricity and the consumption of the RO plant exists. Therefore a chronological perspective is introduced where the current point of time is represented with the value of the parameter “counter”. Furthermore, it is assumed that the RO plant only has the information about the real electricity production cost in the “present”, which corresponds to t with the value of “counter”. This price is determined from the fuel costs of the DG, as PV electricity is seen as a source with zero variable costs:

$$\text{P}_{\text{t}}^{\text{RO}} = \frac{\text{diesel}_{\text{t}} \cdot \text{C}^{\text{diesel}}}{\text{E}_{\text{t}}^{\text{demand}}} \qquad \in \text{t} = \text{counter} \tag{3.29}$$

The actual resulting price for the regarded time step results from the optimization of the RO plant and is determined after the optimization:

$$\text{P}_{\text{t}}^{\text{RO}} = \frac{\text{diesel}_{\text{t}} \cdot \text{C}^{\text{diesel}}}{\text{E}_{\text{t}}^{\text{demand}} + \text{e}_{\text{t}}^{\text{RO}}} \qquad \in \text{t} = \text{counter} \tag{3.30}$$

The “future” prices, meaning p^t with values of t higher than “counter”, are a prediction based on the past prices, meaning p^t with values for t lower than “counter”, of the corresponding moment of the last three days. For achieving a dependency between the scheduling and the price signal and thus a somehow smart scheduling of the RO plant, the actual resulting prices like presented in (3.30) are used for the price prediction:

$$P_t^{RO} = {}^1\!/_3 \cdot P_{t-96}^{RO} + {}^1\!/_3 \cdot P_{t-188}^{RO} + {}^1\!/_3 \cdot P_{t-272}^{RO} \qquad \forall t > \text{counter} \tag{3.31}$$

In conclusion, the optimal decentral control of the RO plant is obtained by conducting an optimization for each "current" time steps. The counter is thereby used to "walk" down the timeline. This results in an approach with as many optimizations as time steps. The initial price signal for the first optimization is a mean price resulting from the total ratio of DG electricity and PV electricity for the whole year from the global optimization. Therefore, the decentral operation approach first has to "adjust" itself and learn from the first scheduling of the RO plant. The decision for the point of time, meaning e_t^{RO} with t equal to "counter", and the deriving values of the other parameters are saved in auxiliary parameters and used as input data for the next optimizations along the timeline.

3.4 Sensitivity analysis and identification of uncertain parameters

All parameters, either system parameters or input data, are exposed to uncertainty. For example, the electrical demand can increase due to new electrical consumers, the solar irradiation can increase or decrease due to changes in the microclimate or the efficiency of the DG can decrease due to wear and tear. These changes have an influence on the optimization model, especially its results on the total costs, the sizing of the system components and the corresponding system control. The parameters differ in their deviation and can be restricted by empirical values and estimations. The investigation of the variation of the parameters and their restrictions is the first step in the identification of uncertain parameters. An sensitivity analysis of the parameters is executed subsequently, whereby the influence of the variation of the parameter on the optimization results are regarded (Campolongo, Saltelli, & Cariboni, 2011). This is done with a simple One Factor At a Time (OAT) method. One parameter is changed and its influence on the outcome of the optimization is calculated, while all other parameters remain at their initial values, called the working point. The parameter is set back to its initial value, and the influence of the next parameter is determined accordingly. The results of interest are the total costs. The analysis is done with the energy system resulting from the optimization for the reference scenario, thus with predefined PV and BS sizes. The reason is that the investment decisions are made in the beginning of the considered time period. Hence, the influence of the uncertain parameters on the chosen optimal system is of major interest. The uncertain parameters are ranked by the resulting change of the total costs of the considered deviations in descending order. In this way, the most important uncertain parameters for the optimized energy supply system can be identified. Although already more advanced techniques are presented and used in modelling practices to identify additional interferences among the parameters, this approach is seen as sufficient in this thesis, since the model is developed strictly linear and additive (Saltelli & Annoni, 2010). Thus, a global sensitivity analysis is achieved also with the OAT analysis.

4 Case study: Ha’apai, Tonga

With the presented model, a case study is conducted for the islands of Lifuka and Fao, which are part of the island group Ha’apai, belonging to the Kingdom of Tonga. Tonga is located in the south pacific, in the north of New Zealand. It consists of four island groups (Tongatapu, Ha’apai, Vava’u and Niuas) with 176 islands, 36 of them inhabited. The climate is tropical with a warm wet season from November to April and a colder dry season from May to October ("Climate Summary of Tonga," 2015). The total population is estimated to be around 103,000, with 73% living on the biggest island Tongatapu, followed by Vava’u with 15%, Ha’apai with 6%, ‘Eua with 5% and Niuas with 1% ("Census of Population and Housing," 2013). 77% of the population is considered to live in rural areas. Tonga has a small economy, remittances and agriculture activities contribute the most to the GDP. However most of the food needs to be imported and agriculture products are the main export earnings (Mofor et al., 2013). 89% of all households are connected to the electricity grid. Electricity on the larger islands is provided by *Tonga Power Ltd* (TPL), a state-owned enterprise which runs DGs with a total capacity of 16.5 MW. Most of the grid-supplied electricity is generated with imported diesel fuel and so imported fuel makes up around 22 % of the total annual imports (Finau, 2014). Therefore a ten year work plan, the *Tonga Energy Road Map* (TERM) 2010-2020, has been developed to reduce the dependency on imported fuel and the fluctuating oil price ("TONGA ENERGY ROAD MAP (TERM) 2010-2020," 2010). Several activities related to TERM in the electricity supply sector have been already implemented, like the grid-connected 1.3 MW_P and 1 MW_P PV stations on Tongatapu or the 500 kW_P PV station on Vava’u. The *Tonga Water Board* (TWB) is responsible for the water supply in the urban centers of the large islands. The water demand is mostly satisfied by groundwater in the form of freshwater lenses and by collected rainwater ("National Integrated Water Resource Management Diagnostic Report: Tonga," 2007).

4.1 Background Lifuka & Foa, Ha’apai

Ha’apai is an island group in the center of the Kingdom of Tonga, around 170 km north of Tongatapu and 130 km to the south of Vava’u. The two neighboring islands, Lifuka and Foa, are the two biggest islands of Ha’apai and have a total population of around 4500. They are linked with a street and share the same electricity network and power supply run by TPL. The locations of the consumers and possible locations of the system components are displayed in Fig. 7. All presented data concerning the energy supply system and solar irradiation have been generously provided by TPL and represent data of the year 2013.

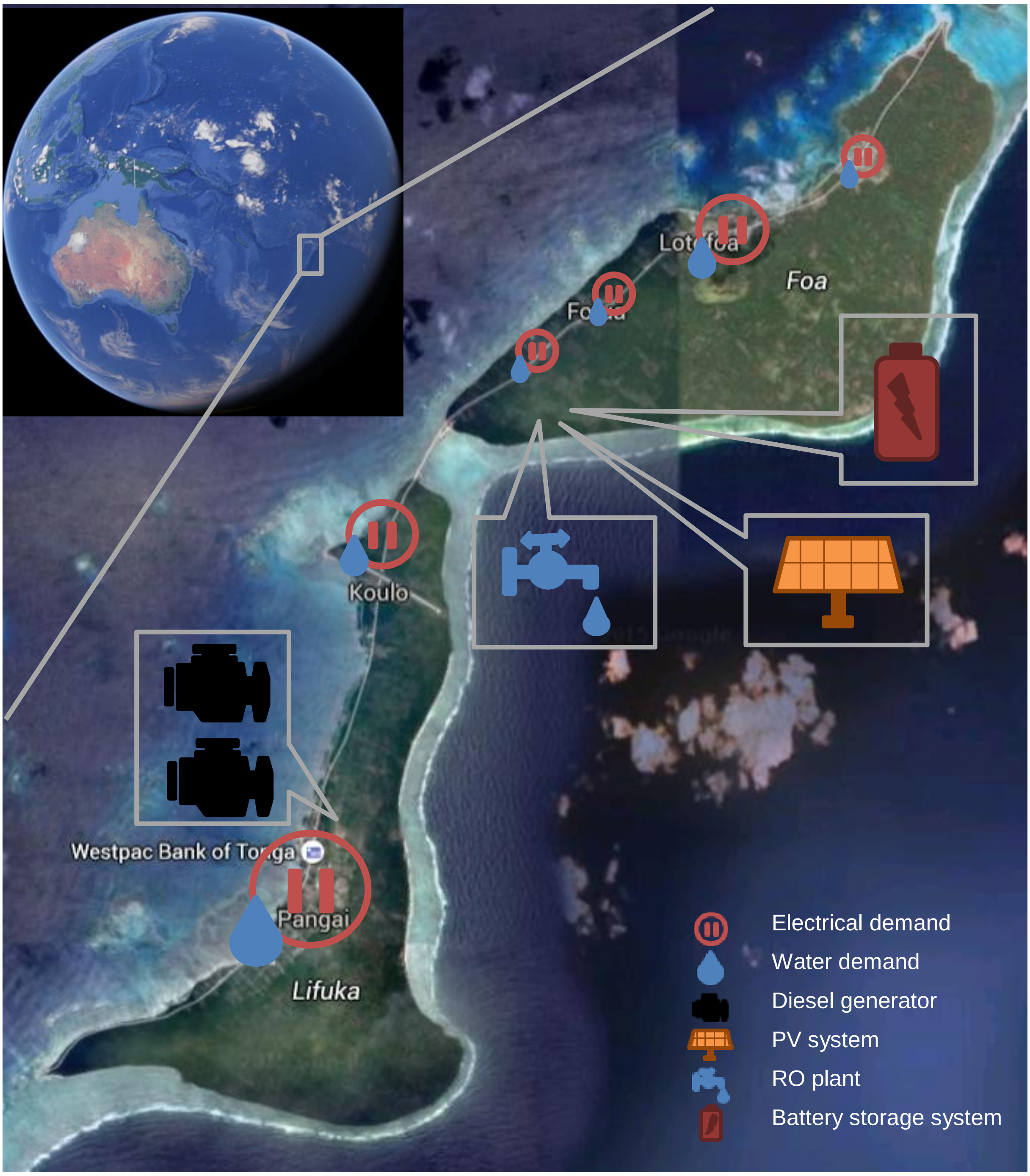

Fig. 7 Map of Lifuka and Foa with the domestic demands and possible locations for the system components of the isolated grid (Google Maps, 2015)

4.2 Electricity demand

TPL supplies around 1000 customers who have an average consumption of 120 kWh per month, per customer according to meter readings. In addition to that TPL supplies the biggest consumers, which are the communications operators, *Tonga Communications Corporation* and *Digicel*, the chapels, TWB water pumps, the hospital and the high schools. The energy produced by TPL in the year 2013 for each day is shown in Fig. 8. It shows a very consistent electricity production for the whole year, although slightly higher in the warmer period from December to April. Furthermore, differences for weekdays and weekends are observable. The received data from TPL have several missing values. Those are linearly interpolated either from the values of the next time step or for larger gaps even for the corresponding day of the next week. As a consequence, the data for the whole August are more or less weekly repeated.

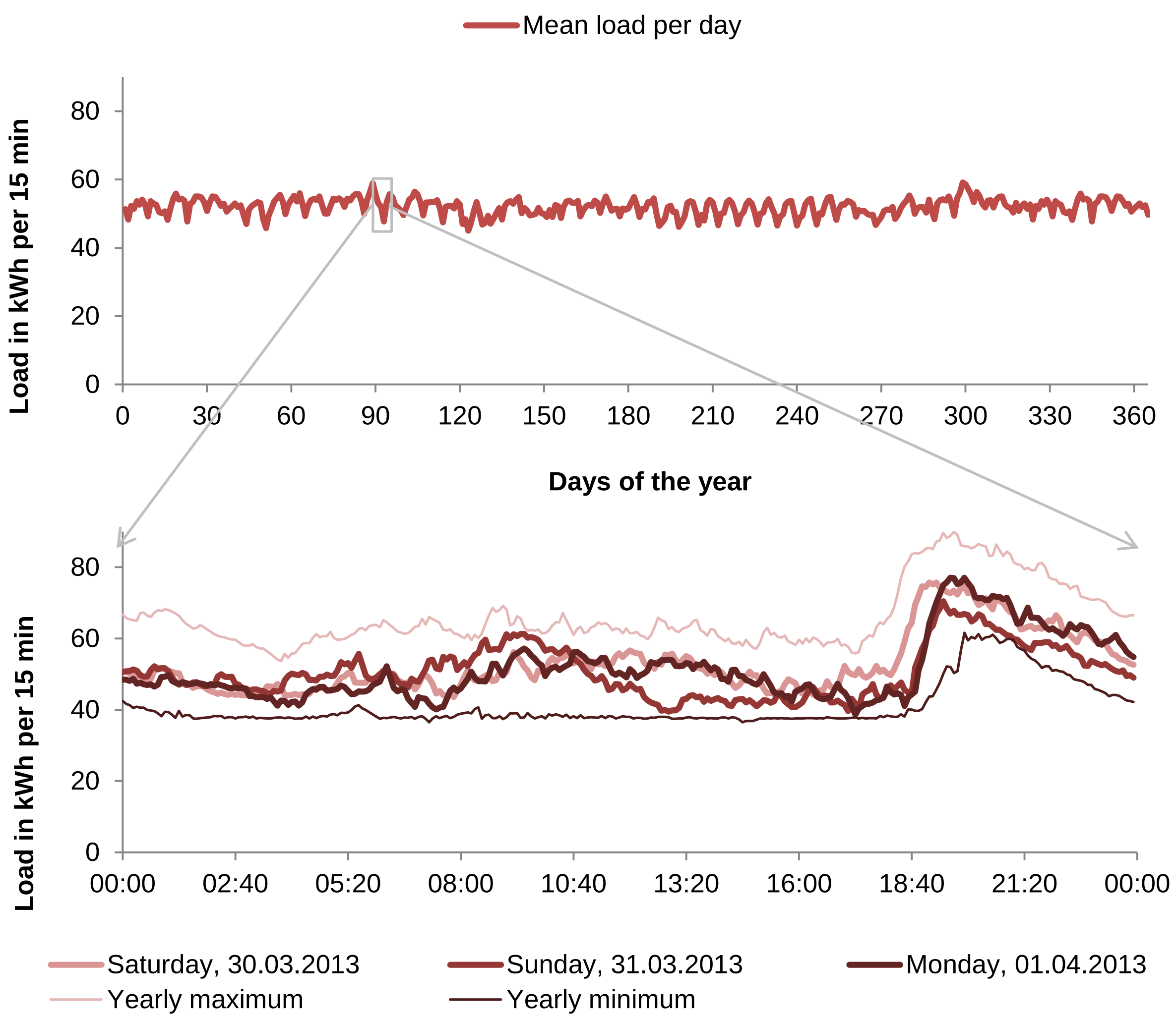

Fig. 8 Yearly and detailed load profile for Lifuka and Foa

Moreover, the data for January and half of February are assigned from November and December, because the received data ranges from mid of February 2013 to mid of February 2014. But due to the heavily destructive cyclone Ian in January 2014, the data from January 2014 onwards are not representative. The load curve of Lifuka and Foa is characterized by a mean load of around 200 kW (50 kWh per 15 min), with a base load of 150 kW (38 kWh per 15 min) and a peak load up to 350 kW (88 kWh per 15 min) in the evening hour. As displayed in Fig. 8, workdays and holidays like Sundays are characterized by a slightly different load shape. During the week, the offices of the communication corporations and the schools add load in the morning and afternoon hours. Common to both is the high evening peak around 20:00 primarily due to lighting and cooking. Saturdays are very similar to workdays.

4.3 Electricity supply system

The current electricity is supplied by two DG with a total capacity of 186 kW each from the type *Cummins NT855*. The DG are specified with a fuel consumption of 0.210 kg/kWh, which results in 0.25 l/kWh assuming a density of 0.840 kg/l for diesel fuel. This value corresponds to $\mathrm{F}^{\mathrm{DG,A}}$. For the model, one DG with a total capacity of 372 kW is considered. Two DG would be modeled with two equation of 3.7b, both with the issue of diesel consumption in idle mode, or with two equation of 3.7c in the milp case, which would increase the computational effort drastically.

Table 2 Technological input parameters for the DG

Parameter	Cummins NT855
$\mathbf{RP^{DG}}$	372 kW
$\mathbf{F^{DG,A}}$	0.25 l/kWh
$\mathbf{L^{DG}}$	30 %
$\mathbf{F^{DG,B}}$	0.239 l/kWh
$\mathbf{F^{DG,C}}$	0.011 l/kW
$\mathbf{C^{diesel}}$	1.2 $/l

Therefore the two DG are considered as one DG with a minimal possible load of 47 kW, which corresponds to a quarterly loaded single DG with an additional fuel consumption of 30% (see Fig. 4.). This results in 0.239 l/kWh for $\mathrm{F}^{\mathrm{DG,B}}$ and 0.011 l/kW for $\mathrm{F}^{\mathrm{DG,C}}$. A constant diesel fuel price for the case study is assumed. The fuel price is set to 1.2 $/l, like published by the government for September 2015. Table 2 summarizes all input data regarding the DG.

4.4 Solar irradiation and PV system

As no recent high-resolution data for Ha'apai are available, the solar irradiation data on an hourly basis of the Maama Mai solar facility on Tongatapu are utilized. The data are linearly interpolated to the required resolution of 15 min steps. Because Tongatapu is located 170 km in the south of Ha'apai, the actual irradiation should be slightly higher, but as stated in the IRENA report for Tonga in 2013, the differences for the whole island Kingdom should not be considerable. Tonga has a high solar resource in general for all months. It is to notice that the irradiation is higher during the warm period when the sun stands high on the horizon with around 1000 W/m². It decreases from March on to about 800 W/m² from May to August. The temperature data are based on averages measured from 1971-2000 at the Salote Pilolevu airport on Lifuka ("CLIMATOLOGICAL INFORMATION – SALOTE PILOLEVU AIRPORT (HAP)," 2006). The data contain daily minimal and daily maximum values for each month that are shown in Table 3. The maximal temperature is assumed from 13:00 to 16:00 o`clock and the minimal temperature from 20:00 to 06:00. The hours between are calculated with a linear interpolation.

Table 3 Average maximal and minimal temperatures of Lifuka

Month	Jan	Feb	Mar	Apr	May	Jun	Jul	Aug	Sep	Oct	Nov	Dec
Average maximal temperature	29.5	30.0	29.8	28.9	27.4	26.4	25.8	25.6	25.9	26.9	28.0	28.8
Average minimal temperature	23.8	24.1	24.1	23.2	22.0	21.2	20.0	19.9	20.3	21.3	22.5	23.3

For the computations with the IIP PV program, a standard multi-crystalline silicone PV module with an efficiency of 16.4% under standard test conditions is selected. The alignment of the module is optimized and should happen with an inclination of 16.3% towards north. For a capacity of 1 kW_P, a module area of 6 m² is needed. The energy produced from a system with 1 kW_P for each day in 2013 is shown in Fig. 9. As already mentioned, the average produced solar energy is the lowest from May to August. The high distortions in February and March are also remarkable. Those occur due to heavy rainfall, because these two months are the wettest months of the year.

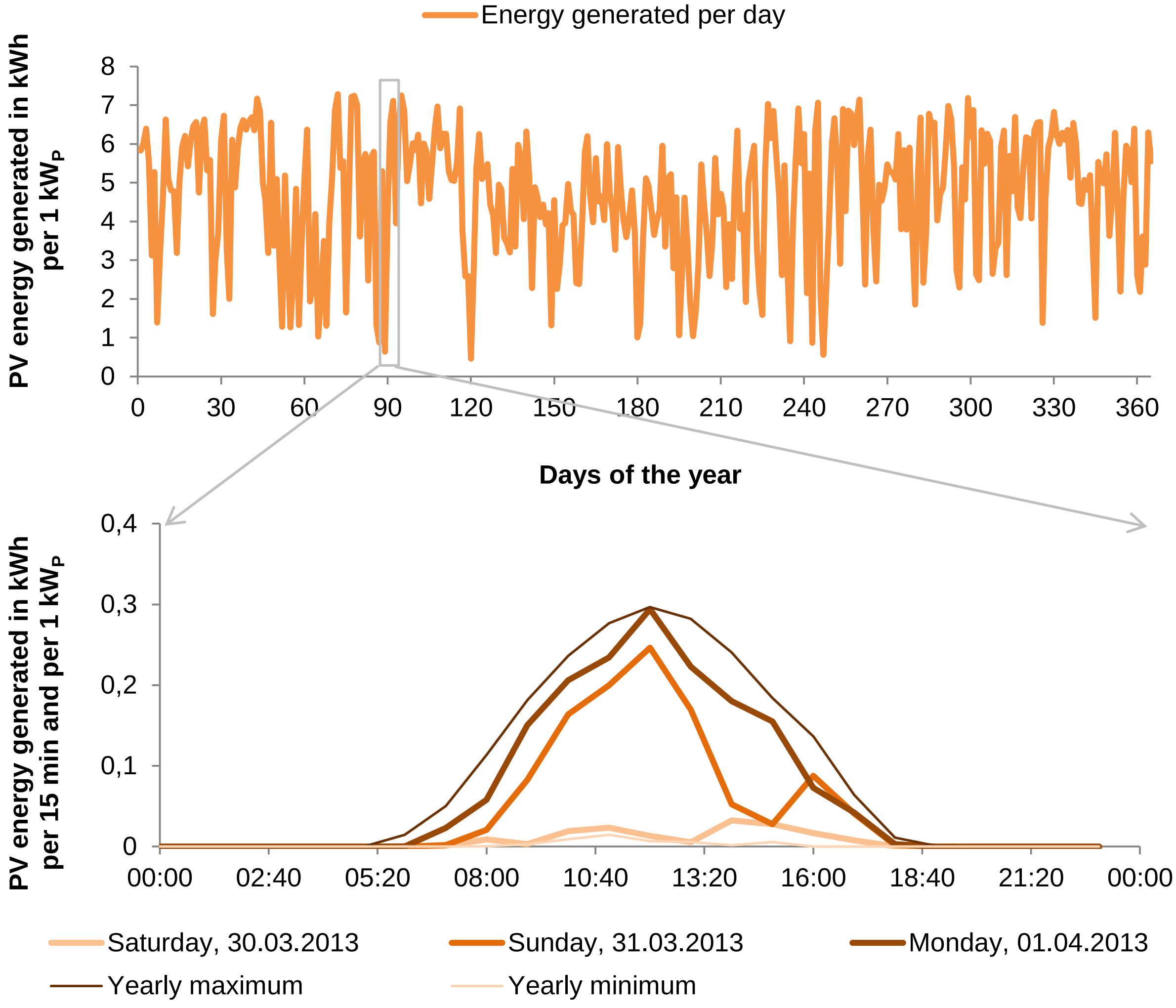

Fig. 9 Generated energy of a PV System with 1 kWP in Tongatapu

The current price of a PV system on Tonga with 1 kW_P is roughly about 2,500 $ as communicated by TPL. The life time and project time of the PV system is estimated at 20 years with an interest rate of 10%. The input parameters for the PV system are shown in Table 4.

Table 4 Technological input parameters for the PV system

Parameter	c-Si
Module efficiency	16.4%
$\mathbf{C^{PV}}$	2,500 $/1kW$_P$
$\mathbf{LT^{PV}}$	20 years
$\mathbf{I}$	10%

4.5 Battery storage system

The characteristics of the considered BS system are derived from a lithium-ion battery system which has been offered to the IIP for one of its projects. The price for one battery unit, which offers an energy capacity of 1 kWh and a power capacity of 1 kW, is 1,000 €. However, due to the foreign currency translation and assumed higher costs for transportation and installation in Tonga, a price of 1,200 $ is used. The lithium-ion battery offers a round-trip efficiency of 90% and a deep-discharging level of 90%.

Table 5 Technological input parameters for the battery storage system

Parameter	Lithium-ion battery
$\mathbf{E^{BS,cap}}$	1 kW/unit
$\mathbf{S^{BS,cap}}$	1 kWh/unit
$\mathbf{L^{BS,rte}}$	90%
$\mathbf{L^{BS,dd}}$	90%
$\mathbf{L^{BS,sdl}}$	0%
$\mathbf{C^{BS}}$	1200 $/unit
$\mathbf{LT^{PV}}$	10 years
$\mathbf{I}$	10%

The self-discharging losses for a lithium-ion battery in the regarded time periods are negligible. Because no real long-term experiences are known for the operation of lithium-ion battery systems, the life time of the BS is equal to the warranty of the manufacturer, which is ten years. Again an interest rate of 10% is chosen. All used data for the BS are shown by Table 5.

4.6 Water demand

The water supply is operated by the *Tonga Water Board* (TWB). On Lifuka and Foa, the water is extracted from a groundwater lens with water pumps partly powered by electricity, diesel fuel or recently also solar power. The *South Pacific Applied Geoscience Commission* (SOPAC) has carried out several studies examining Tonga´s water supply. For the Nuku'alofa area on Tongatapu, the average domestic water demand is estimated 0.1 m³ per day per person ("National Integrated Water Resource Management Diagnostic Report: Tonga," 2007). With 4500 inhabitants, this results in 450 m³ water per day for Lifuka and Foa. It is considered, however, that half of the demand is supplied by the RO plant and the other half by the existing groundwater pumps. The water demand is assumed to be consistent for the whole year, because no data for a more precise temporal distinction are available. During the day, from 07.45 to 19.30 o`clock, the water demand is estimated three times higher than during the night. For Ha'apai, the SOPAC report states that the groundwater is significantly contaminated due to septic tanks, pit latrines, pigs and over-pumping. A solution could be a seawater RO system, which can guarantee a clean water supply without further stressing the freshwater lens of the island.

4.7 Desalination system and water storage

The used desalination system is a modular and variable RO system from *ENERCON* ("ENERCON DESALINATION SYSTEMS,"). A module has one water pump for the RO process and can desalinate 175-350 m³ seawater per day. The specific energy consumption is 2.5 kWh/m³ (Paulsen & Hensel, 2007). For the case study, a two module system is chosen. This results in a rated power of 72.3 kW and a desalination capacity of 700 m³/day. The infinitesimal loss factor is set to 0.01%. For the water storage, a water tank with a storage capacity of two times the daily water consumption is assumed. All data are listed in Table 6.

Table 6 Technological input parameters for the desalination system and the water storage

Parameter	**Lithium-ion battery**
$\mathbf{RP^{RO}}$	72.97 kW
$\mathbf{F^{RO}}$	2.5 kWh/m³
$\mathbf{L^{RO}}$	0.01 %
$\mathbf{S^{WS,max}}$	2 days

5 Results and discussion

The optimal energy supply system with the presented input parameters for the isolated grid of Ha'apai is studied. The different modeling approaches for the DG and the RO system are compared. Several scenarios for the energy supply system, the RO system and the BS are defined. The decentralized control approach with a price signal for the RO system is calculated and compared to the centralized control obtained by the optimization for the entire system. The identification of the most important parameters and the sensitivity analysis are presented afterwards.

5.1 Optimal energy supply system

The results of the optimization for the studied isolated grid on Ha'apai are presented in Table 7. The optimized system has to supply the yearly static energy demand of 1,822,158 kWh and an additional 205,313 kWh for the RO system. The optimal installed PV system shows a capacity of 304.4 kW_P and supplies 23.8% of the yearly energy demand. PV power needs to be curtailed regularly as the capacity exceeds the average load during midday and the maximal possible RO load, which are about 200 kW and 73 kW. The proportion of the dumped load to the overall PV generated energy is 6.9%. The excess energy cannot be stored as no BS is installed. The total costs of the yearly energy supply sums up to 575,159 $, while the annuity of the PV system accounts for 89,403 $ and the diesel fuel cost accounts for 485,756 $. This results in a LCOE, which describes the ratio of the total costs over the total supplied energy, of 0.284 $/kWh.

Table 7 Results of the optimal energy supply system for Ha'apai

Scenario	$\sum e_t^{DG}$ (kWh)	$capacity^{PV}$ (kW_p)	$\sum e_t^{PV}$ (kWh)	$\sum e_t^{DL}$ (kWh)	% of used e_t^{PV}	% of e_t^{DL} on e_t^{PV+DL}	$capacity^{BS}$ (units)	$cost^{total}$ ($)	$cost^{PV}$ ($)	LCOE ($/kWh)
ES3/RO3	1,545,776	304.4	481,694	35,532	23.8%	6.9%	-	575,159	89,403	0.284

The energy supply and demand characteristics for each month are displayed in Fig. 10. As expected, the dumped load is the lowest during the month of May, June and July, which also have the lowest solar irradiation. The required energy for the desalination process is distributed very consistently over the month. The reasons are the comparatively small storage which can last only two days and the need to satisfy the water demand.

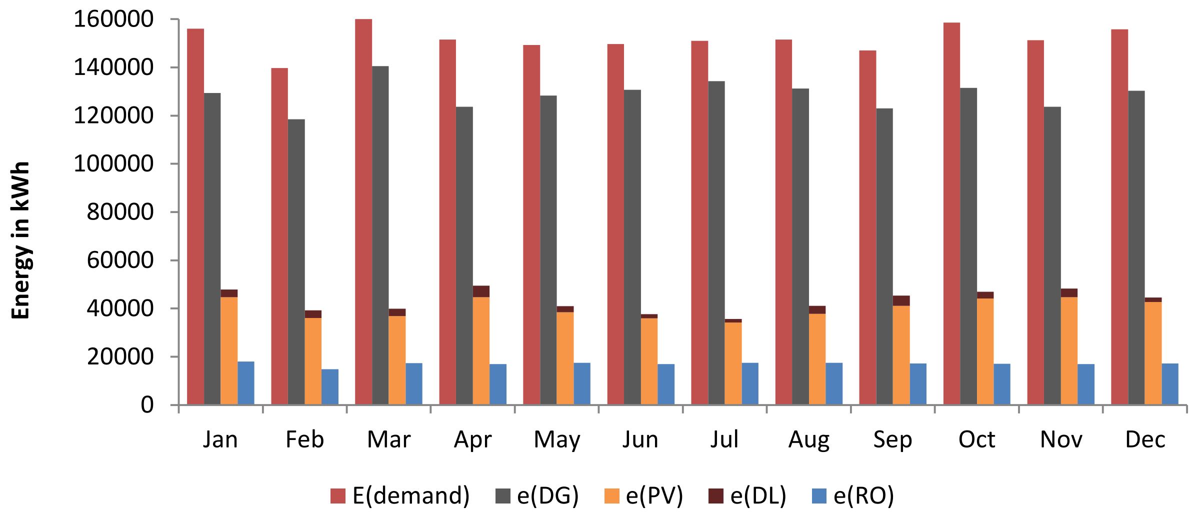

Fig. 10 Electrical demand and optimized energy supply and RO operation for each month

The operation of the system components for two different weeks is depicted in Fig. 11 and Fig. 12. Fig. 11 shows a week in the beginning of February with a high and very constant solar irradiation. During midday and high PV power generation, the DG mostly runs on its minimal loading capacity.

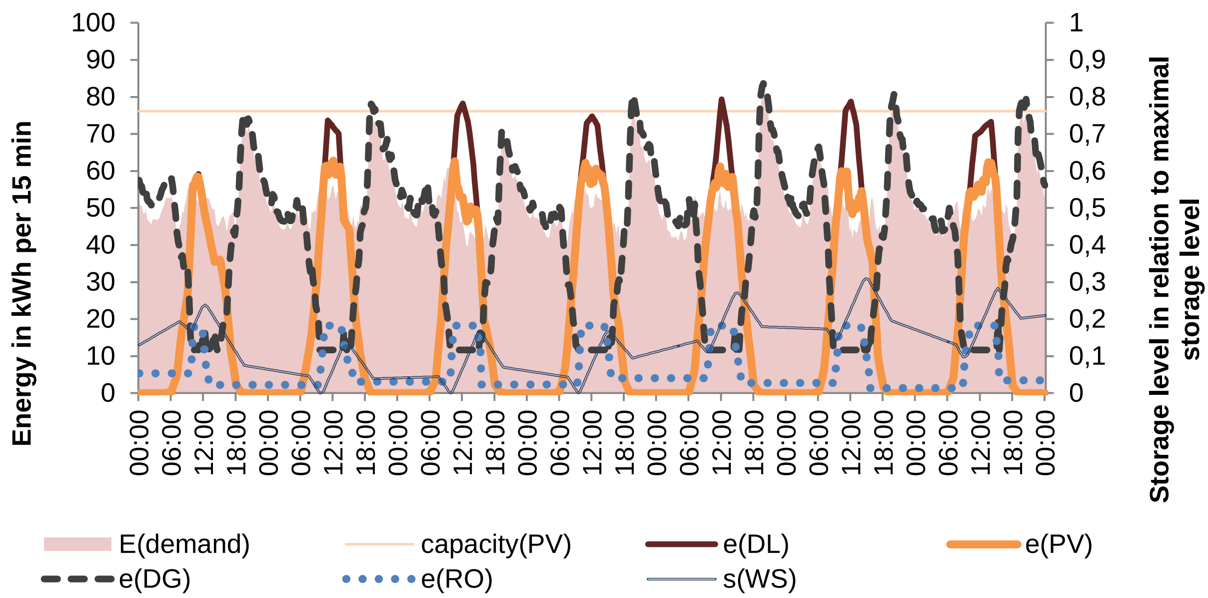

Fig. 11 Energy supply/demand and operation of the RO system for a week in February with high and constant PV power production

In nearly the same period, the RO system simultaneously increases its energy consumption up to its rated power and thus tries to utilize as much PV power as possible. Between the sunshine hours the water desalination is scaled down to values mostly of 2 to 3 kWh per 15 min. The water storage is not filled above 30% of its capacity and is emptied in the morning of each day. This similar operational characteristic for each day is due to the constant solar radiation. The week for the mid of July with comparably low and fluctuating solar irradiation, displayed in Fig. 12, shows a very different operational strategy for the RO system and a different usage of the water storage. The RO plant increases the production of drinking water on the second day and keeps it up till the fourth day of the week to fill the water storage. Hence, it is possible to nearly shut down the desalination process on the fifth, sixth and seventh day which are very cloudy with low PV power production.

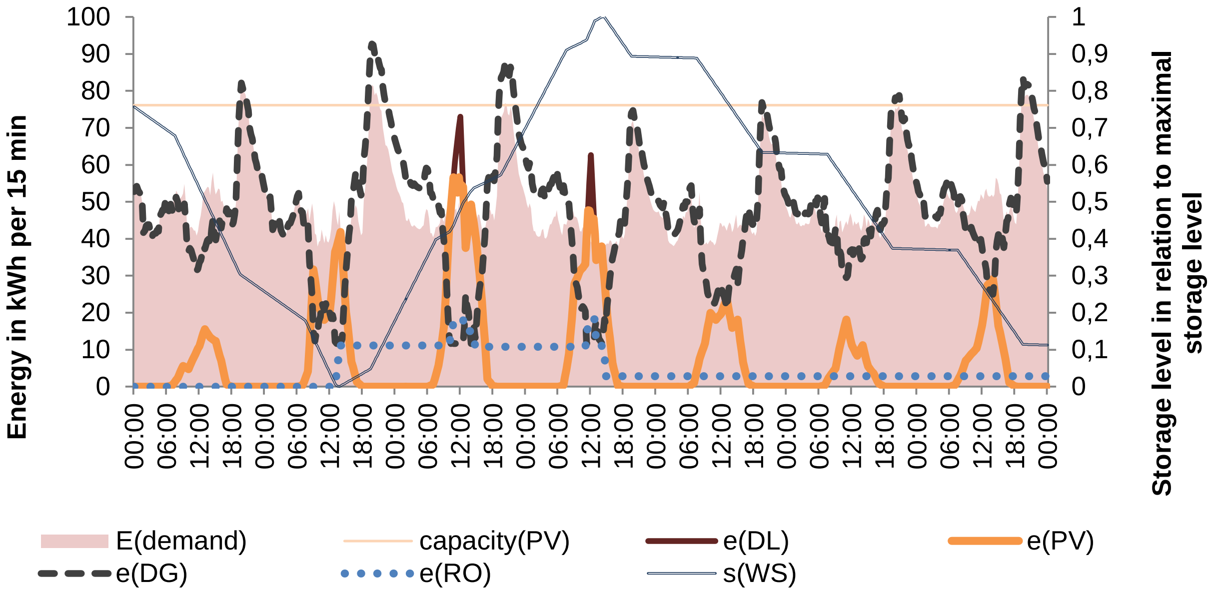

Fig. 12 Energy supply/demand and operation of the RO system for a week in July with low and fluctuating PV power production

5.2 Integration of PV power in different scenarios

Four different energy supply scenarios for the integration of PV power are considered and compared:

- ES0: business as usual, no investment possibilities in PV and BS, no RO system; static energy demand of 1,822,158 kWh
- ES1: investment possibilities in PV and BS, no RO system; static energy demand of 1,822,158 kWh

- ES2: investment possibilities in PV and BS; static energy demand of 1,822,158 kWh + static continuous RO demand of 205,313 kWh
- ES3 (reference scenario): investment possibilities in PV and BS; static energy demand of 1,822,158 kWh + variable RO demand of 205,313 kWh

In scenario ES0 and ES1, it is considered that the water demand is satisfied by groundwater and collected rainwater. The resulting optimal energy supply system and the corresponding costs are summarized in Table 8. As might be expected, the integration of a PV system leads to a reduction of the total costs of about 5.1%. Approximately 17.6% of the energy demand is satisfied by the PV system instead of the expensive DG. Again, not all PV generated electricity can be consumed and thus the dump load makes up 7.2% of the total generated PV energy. The LCOE decreases from 0.318 \$/kWh to 0.298 \$/kWh.

Table 8 Results of the PV integration for Ha'apai

Scenario	$\sum e_t^{DG}$ (kWh)	$capacity^{PV}$ (kW_p)	$\sum e_t^{PV}$ (kWh)	$\sum e_t^{DL}$ (kWh)	% of used e_t^{PV}	% of e_t^{DL} on e_t^{PV+DL}	$capacity^{BS}$ (units)	$cost^{total}$ (\$)	$cost^{PV}$ (\$)	LCOE (\$/kWh)
ES0	1,822,158	-	-	-	-	-	-	565,117	-	0.310
ES1	1,496,284	206.7	325,874	25,303	17.9%	7.2%	-	532,246	60,701	0.292
ES2	1,651,758	237.8	375,712	28,337	18.5%	7.0%	-	586,028	69,840	0.289
ES3	1,545,776	304.4	481,694	35,532	23.8%	6.9%	-	575,159	89,403	0.284

The introduction of the RO system adds a yearly load of 205,313 kWh. In the continuous operating case, this corresponds to an additional load of 5.9 kWh per 15 minutes. Thus, the size of the PV system increases from 206.7 kW_P in ES1 to 237.8 kW_P in ES2. Additionally, the LCOE decreases slightly to 0.289 \$/kWh, because the DG operates with a higher efficiency and more PV energy is utilized. The optimal energy supply for a system with a variable operating RO plant, shows the highest capacity of PV power with 304.4 kW_P. The ratio of consumed PV electricity increases to 23.8% and the ratio of unused PV power decreases to 6.9%. This leads to a further reduction of the LCOE to 0.284 \$/kWh and to a reduction of the total costs of 1.9% compared to ES2. In conclusion, the optimal PV system for the isolated grid of Ha'apai is designed in such way that an excess of PV generated electricity of about 7% exists. For all scenarios, the installation of a BS system is too expensive and not beneficial.

5.3 Integration of desalination as a flexible load

Again different scenarios are defined to analyze the impact of the integration of a flexible RO system and their results are listed in Table 9. The rated power of the variable RO plant is like previously defined about 73 kW:

- RO2: integration of variable RO plant; PV system with 237.8 kW_P (see ES2)
- RO3 (reference scenario): see ES3
- RO4: double the water demand (450 m³ per day) for the standard variable RO system; PV size optimized
- RO5: standard water demand (225 m³ per day) and RO system with double the capacity; PV size optimized
- RO6: double the water demand (450 m³ per day) and RO system with double the capacity; PV size optimized

Table 9 Results for the integration of a flexible RO desalination plant for Ha'apai

Scenario	$\sum e_t^{DG}$ (kWh)	$capacity^{PV}$ (kW_p)	$\sum e_t^{PV}$ (kWh)	$\sum e_t^{DL}$ (kWh)	% of used e_t^{PV}	% of e_t^{DL} on e_t^{PV+DL}	$capacity^{BS}$ (units)	$cost^{total}$ ($)	$cost^{PV}$ ($)	LCOE ($/kWh)
RO2	1,627,573	237.8	399,896	4,153	19.7%	1.0%	-	579,084	69,840	0.286
ES3/RO3	1,545,776	304.4	481,694	35,532	23.8%	6.9%	-	575,159	89,403	0.284
RO4	1,751,087	304.4	481,694	35,532	21.6%	6.9%	-	634,112	89,403	0.284
RO5	1,444,452	357.8	583,019	24,783	28.8%	4.1%	-	561,720	105,058	0.277
RO6	1,595,346	402.4	637,435	46,285	28.0%	6.8%	-	618,171	118,181	0.277

The installation of a flexible operating RO system leads to a radical decrease of unused PV electricity from 7.0% in ES2 to 1.0% in RO2. Thus, also the total costs of the energy supply and the LCOE decreases slightly by 1%. In scenario RO4 double the water demand is covered by the RO system. Compared to RO3, the results of RO4 reveal that the PV system size is optimized for the given RO capacity. The additional energy demand of the RO system for satisfying the water demand in RO4 is supplied by the DG. This leads to a decrease of the percentage of PV energy. The usage of a RO plant with twice the capacity results in a PV size of 357.8 kW_P in RO5, which makes up 28.8% of the total energy supply. With 4.1% for the dumped PV electricity, this scenario introduces a new characteristic value. The optimal energy supply system for in RO6 with double the RO plant capacity and double the water demand has an even higher PV capacity, thus a higher penetration of PV power, a lower LCOE, but again a percentage of unused PV electricity around 7.0%. Important for the integration of the flexible RO system and the corresponding optimal PV system are the maximal available flexible capacity and the degree of flexibility which can be defined as ratio of demand to capacity, resulting in the effective operating time. For RO2, RO3 and RO6, the energy demand for the water desalination process is about 563 kWh per day. With a rated power of 73 kW for the RO plant, a minimal operating time of 7.7 hours is achieved. RO4 has double the demand and thus double the minimal operating time of 15.4 hours. The least effective operating time has RO5 with 3.9 hours.

5.3.1 Operational characteristics of the flexible desalination system

When the optimized operational characteristics of the RO system are analyzed, it is to notice that the RO system often operates with a low capacity factor between the sunshine hours. As presented in chapter 4.7, the considered RO system consists of two modules with an operating range from 4.6 kWh per 15 min to 9.2 kWh per 15 min, resulting in a total system with an operating range from 4.6 kWh per 15 min to 18.4 kWh per 15 min. However the optimized operational characteristic often falls below this minimal load, like it also is displayed in the weeks in Fig. 12 and Fig. 13. The reference scenario is modeled with the unrestricted operating RO system as a lp model. Thus the RO system is operating 126.0 days in the invalid range. For a comparison, scenario RO3bin1 and RO3bin2 are defined, which are both optimized as a milp model with a restricted operating RO system:

- RO3bin1: investment possibilities in PV and BS; static energy demand of 1,822,158 kWh + variable RO demand of 205,313 kWh; RO system modeled as milp

- RO3bin2: fixed PV system with 304.4 kWP (see ES3/RO3); static energy demand of 1,822,158 kWh + variable RO demand of 205,313 kWh; RO system modeled as milp

RO3bin1 is solved in 10 hours and 50 min with 0.1% for the tolerance gap, while RO3bin2 is solved in around 40 min, also with 0.1% for the tolerance gap. The lp approach of ES3/RO3 is solved in less than 10 min. The operational characteristics for the whole year are summarized in Table 10. The resulting differences are obvious. For the lp approach, the RO system operates 126 days of the year in the invalid operation range. This time interval is distributed in the over the valid operation areas in RO3bin1 and RO3bin2. However, the period of the full load operation only differs slightly in all scenarios.

Table 10 Operational characteristics of the lp and milp RO modelling approaches

Scenario	System shut down ($e_t^{RO} = 0$)	Invalid operation range ($0 < e_t^{RO} < 4.6$)	Valid variable operation range ($4.6 < e_t^{RO} < 18.4$)	Full load operation ($e_t^{RO} = 18.4$)
RO3	68.8 days	126.0 days	136.2 days	34.0 days
RO3bin1	126.3 days	-	203.7 days	35.0 days
RO3bin2	122.9 days	-	208 days	34.1 days

The differences for the key figures of the two models presented in Table 11 are marginal. RO3bin1 shows a slightly lower PV capacity. Nevertheless, RO3bin2 with the predefined PV size results in less total costs and therefore it can be concluded that the optimal energy supply system for the operational restricted RO system is also 304.4 kWP.

Table 11 Results of of the lp and milp RO modelling approaches

Scenario	$\sum e_t^{DG}$ (kWh)	$\mathrm{capacity}^{PV}$ (kW_p)	$\sum e_t^{PV}$ (kWh)	$\sum e_t^{DL}$ (kWh)	% of used e_t^{PV}	% of e_t^{DL} on e_t^{PV+DL}	$\mathrm{capacity}^{BS}$ (units)	cost^{total} ($)	cost^{PV} ($)	LCOE ($/kWh)
ES3/RO3	1,545,776	304.4	481,694	35,532	23.8%	6.9%	-	575,159	89,403	0.284
RO3bin1	1,547,125	303.2	480,346	34,744	23.7%	6.8%	-	575,177	89,034	0.284
RO3bin2	1,545,780	304.4	481,690	35,536	23.8%	6.9%	-	575,160	89,403	0.284

That is why, the linear modeling approach for the RO system is sufficient for this studies, because the computational extra effort for the milp approach does not offer any further understanding of the optimal energy supply system when the restrictions for the RO system are kept in mind.

5.3.2 Economic analysis of the flexible desalination system

As concluded previously, the integration of a flexible operating RO system is offering an economical benefit from the perspective of the energy supply system. For offering flexibility, the RO system has to be designed with an overcapacity, to have an effective operating time less than 24 hours. Higher capacity results in higher flexibility, but also in higher capital costs for installing the RO system. *SYNWATER* is calculating about 1,000 €/(m^3/d) for a similar variable operating RO system (Käufler et al., 2012). As to the BS system, a 20% higher dollar price is assumed, giving 1,200 €/(m^3/d). The annuity factor is given by the operating life with 20 years and the interest rate with 10%. The resulting associated costs for the different RO systems are listed in Table 12.

Table 12 Associated costs of the different RO systems

Scenario	RO capacity (m^3/d)	$\mathbf{cost^{RO}}$ ($)	$\mathbf{cost^{total}}$ ($)	$\mathbf{cost^{total+RO}}$ ($)
ES2	225	31,714	586,028	617,742
ES3/RO3	700	98,666	575,159	673,825

The savings on the energy supply side with a flexible operating RO plant are not enough to compensate the additional capital costs of a RO system with overcapacity. Thus, ES2 results in the scenario with less total costs per year, when the capital costs of the RO system are also taken into considerations.

5.4 Integration of a battery storage system as a flexible load

Although no BS system is chosen in the previous scenarios, the implementation of a BS as a flexible load is also analyzed. Therefore, several system parameters are predefined which are given in the following scenario:

- BS3: fixed PV system with 304.4 kW_P (see ES3/RO3); continuous operating RO plant; constraint to achieve the same PV power utilization ($\sum \mathbf{e_t^{PV}}$=473,225 kWh)

The results of BS3 are listed in Table 13. The scenario with BS are all optimized with the milp model for the DG to realize a possible shut down of the DG.

Table 13 Results of the integration of a BS for Ha'apai

Scenario	$\sum e_t^{DG}$ (kWh)	$\sum e_t^{PV}$ (kWh)	$\sum e_t^{DL}$ (kWh)	% of used e_t^{PV}	% of e_t^{DL} on e_t^{PV+DL}	$capacity^{BS}$ (units)	$cost^{total}$ ($)	$cost^{PV}$ ($)	$cost^{BS}$ ($)	LCOE ($/kWh)
ES3/RO3	1,545,776	481,694	35,532	23.8%	6.9%	-	575,159	89,403	-	0.284
BS3	1,577,700	481,694	35,532	23.4%	6.9%	52.8	593,880	89,403	8,599	0.288

Due to the predefined PV size and PV utilization, the scenario BS3 shows the same values for most of the key figures of the energy supply as ES3. However, the total energy supply in BS3 is 31,924 kWh higher due to the charging and discharging losses of the BS. This additional energy has to be supplied by the DG, hence reducing the percentage of the used PV electricity. The total costs of BS3 increase by 3.3% in comparison to ES3/RO3. The capital costs for the BS only make up 46% of the additional costs, while 54% account for the additional fuel consumption of the DG. The BS is sized to achieve the predefined PV utilization. Its capacity is far too little to take over the responsibility for the grid stability and to realize a shut-down of the DG. An optimization with the milp model with a tolerance gap of 0.1% is solved in about 37 hours and 25 minutes.

5.5 Decentralized integration of the flexible desalination system with a price signal

The results of the decentralized demand response approach for the flexible RO system are presented in Table 14. The scenario for the decentralized integration is defined as:

- DI3: fixed PV system with 304.4 kW_P (see ES3/RO3); Decentral integration of the RO system with an price signal

Table 14 Results of the decentral integration approach of the RO system

Scenario	$\sum e_t^{DG}$ (kWh)	$capacity^{PV}$ (kW_p)	$\sum e_t^{PV}$ (kWh)	$\sum e_t^{DL}$ (kWh)	% of used e_t^{PV}	% of e_t^{DL} on e_t^{PV+DL}	$capacity^{BS}$ (units)	$cost^{total}$ ($)	$cost^{PV}$ ($)	LCOE ($/kWh)
ES3/RO3	1,545,776	304.4	481,694	35,532	23.8%	6.9%	-	575,159	89,403	0.284
DI3	1,545,979	304.4	481,492	35,735	23.8%	6.9%	-	-	-	-

It is remarkable that the resulting key figures of the optimizations are nearly the same for the decentralized optimization approach in PS3 as for the overall system optimization in ES3/RO3. Thus, the corresponding overall costs for the energy supply are also nearly equivalent. This result is very surprising, as the decentralized optimization is not concerning the condition of the other system components in any way. Differences are found in the operational characteristic of the flexible RO system. The summarized values for the whole year are presented in Table 15.

Table 15 Operational characteristics of the decentralized integration of the RO system

Scenario	System shut down ($e_t^{RO} = 0$)	Invalid operation range ($0 < e_t^{RO} < 4.6$)	Valid variable operation range ($4.6 < e_t^{RO} < 18.4$)	Full load operation ($e_t^{RO} = 18.4$)
RO3	68.8 days	126.0 days	136.2 days	34.0 days
DI3	246.9 days	0.7 days	1.0 days	116.4 days

The RO system in DI3 is either operating with full load or is shut down in the most cases. Thus the minimal load restriction for the RO system characteristic is nearly fulfilled. The RO system is just operating 0.7 days in the invalid operation range. The detailed operation of the RO system is shown with the two typical weeks of beginning of February and mid of June in Fig. 13, respectively Fig. 14. Unlike for Figure 11 and Fig 12, the operation of the RO system is very similar for both weeks. When the energy generated by the PV system exceeds the rated power of the RO system, the RO system starts working and increases the water desalination to its rated value. It stops to operate, when the PV power generation is decreasing.

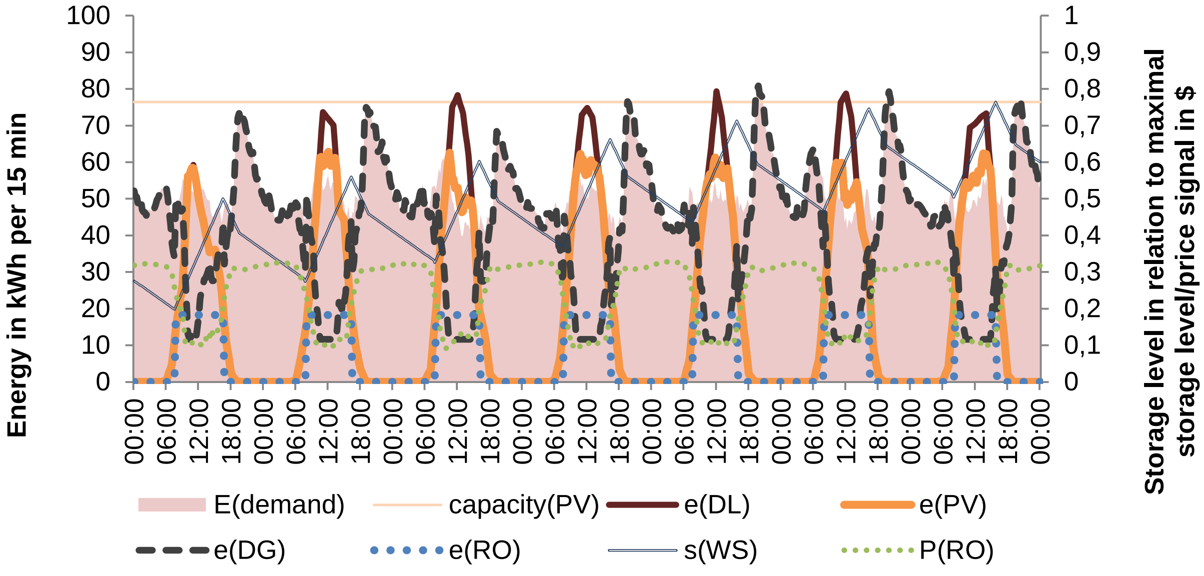

Fig. 13 Energy supply/demand and operation of the decentralized integrated RO system for a week in February with high and constant PV power production

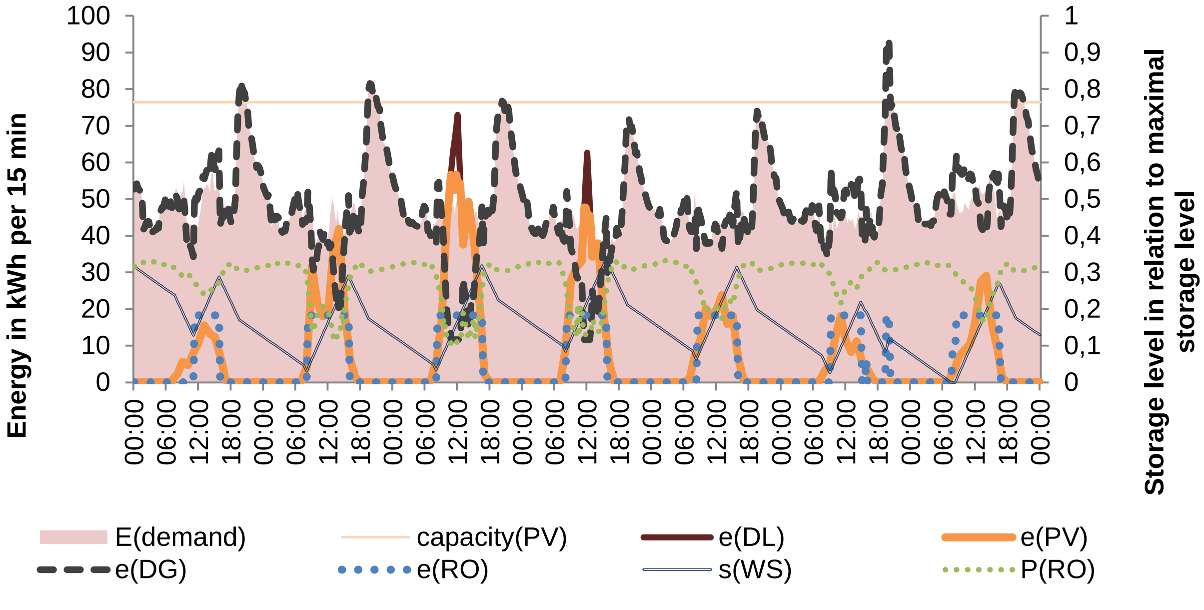

Fig. 14 Energy supply/demand and operation of the decentralized integrated RO system for a week in July with low and fluctuating PV power production

Hence, the RO operation is each day nearly the same, especially in the week of February. As additional information, the resulting price signal is displayed in Fig. 13

and Fig. 14. Exceptions are the first day and the fifth day of the week in July. Due to low PV power generation, the RO system limits the full loaded operation period. On the fifth day, the desalination process is even shifted to the evening peak, because of a low price signal due to the high working efficiency of the DG. This can lead to an overload of the DG. Regarding the whole year, the DG is overloaded 13 times, which corresponds to 3.3 hours. Compared to a whole year, this value is almost negligible. However, it is revealed that additional information on the total system condition for the decentralized integration of flexible loads is necessary. For example, this could be realized by a predefined additional level of information incorporated in the price signal.

5.6 Sensitivity analysis and ranking of uncertain parameters

The variations of the parameters are listed in Table 16. The cost of PV technology can also be much higher in Tonga as stated by TPL. Therefore a price increase of 64% is assumed. Future research and technology improvement could also lead to a reduced PV price, which is considered with a decrease of 32%. The diesel price for Tonga is analyzed by a report of the world bank for the energy supply system of Tonga (Swales, Hughes, & Asseline, 2010). In the high oil price projection, a diesel price of 1.4 $ in 2020 is assumed. Moreover, a negative variance is also taken into consideration as the oil price is generally subject to variations. The report also assumes an increase of the electrical demand of maximal 20% till 2020. The population census in 2013 revealed that the population of Ha’apai is not increasing, because of an outflow of people to the mainland Tongatapu ("Census of Population and Housing," 2013). Thus, a decrease of 8% of the electricity demand also has to be considered. The power production of a PV system is exposed to degradation and to fluctuation of the solar irradiation, therefore an increase of 4% and a decrease of 16% of the PV power production is analyzed (Osterwald, Anderberg, Rummel, & Ottoson, 2002). The specific fuel consumption of the DG is increasing with time and the value communicated by TPL is comparably low (Yamegueu et al., 2011). Hence, an increase of 32% is considered. The same applies to the energy consumption of the RO system. However an increase of 64% is considered, because comparable RO systems show an energy consumption of up to 4 kWh/m^3 (Käufler et al., 2012). The influence of the interest rate has to be analyzed, because it can vary for a developing island state like Tonga, which is exposed to tropical storms like cyclone Ian in 2014. The life time of the PV system undergoes the same risks. The rated power of the DG and RO are assumed to decrease in time, each with 16%. When the groundwater of Ha'apai is further contaminated, the water demand for the RO system could increase drastically. For this analysis, an increase of 128% is considered. All assumed variations are listed in Table 16.

Table 16 Variations of the uncertain parameters

Parameter	Reference value	Maximal value	Minimal value	Maximal variance	Minimal variance
$\mathbf{C^{diesel}}$	1.2 $	1.4 $	1.0 $	+ 16%	- 8%
$\mathbf{C^{PV}}$	2,500 $	4,100 $	1,700 $	+ 64%	- 32%
$\sum \mathbf{E_t^{demand}}$	1,822,158 kWh	2,181,928 kWh	1,749,272 kWh	+ 20%	- 4%
$\sum \mathbf{e_t^{PV+DL}}$	517,226 kWh	537,915 kWh	434,470 kWh	+ 4%	- 16%
$\mathbf{F^{DG,A}}$	0.25 l/kWh	0.33 l/kWh	0.25 l/kWh	+ 32%	0%
$\mathbf{F^{RO}}$	2.5 kWh/ m³	4.1 kWh/ m³	2.5 kWh/ m³	+ 64%	0%
$\mathbf{I}$	10%	16. 4%	3.8%	+ 64%	- 64%
$\mathbf{LT^{PV}}$	20 years	33 years	7 years	+ 64%	- 64%
$\mathbf{RP^{DG}}$	372 kW	372 kW	312 kW	0%	- 16%
$\mathbf{RP^{RO}}$	73 kW	73 kW	61 kW	0%	-16%
$\sum \mathbf{W_t^{demand}}$	82,125 m³	187,245 m³	82,125 m³	+ 128%	0%

The result for the OAT sensitivity analysis and the influence of the uncertain parameters on the annual costs are presented in Fig. 15. It is remarkable, that all parameters except for the time life of the PV system, the electrical demand and the specific fuel consumption of the DG show a linear influence on the annual costs of the energy supply system. In the case of the electrical demand, an increase of 8% of the demand would lead to a loss of the energy supply in peak periods, because the load exceeds the rated power of the DG. The loss of the power supply is assumed to result in high total costs. The degree of influence on the total costs is expressed by the slope of the line. Thus, the electrical demand, the specific fuel consumption of the DG and the price for diesel show by far the highest influence on the total annual costs.

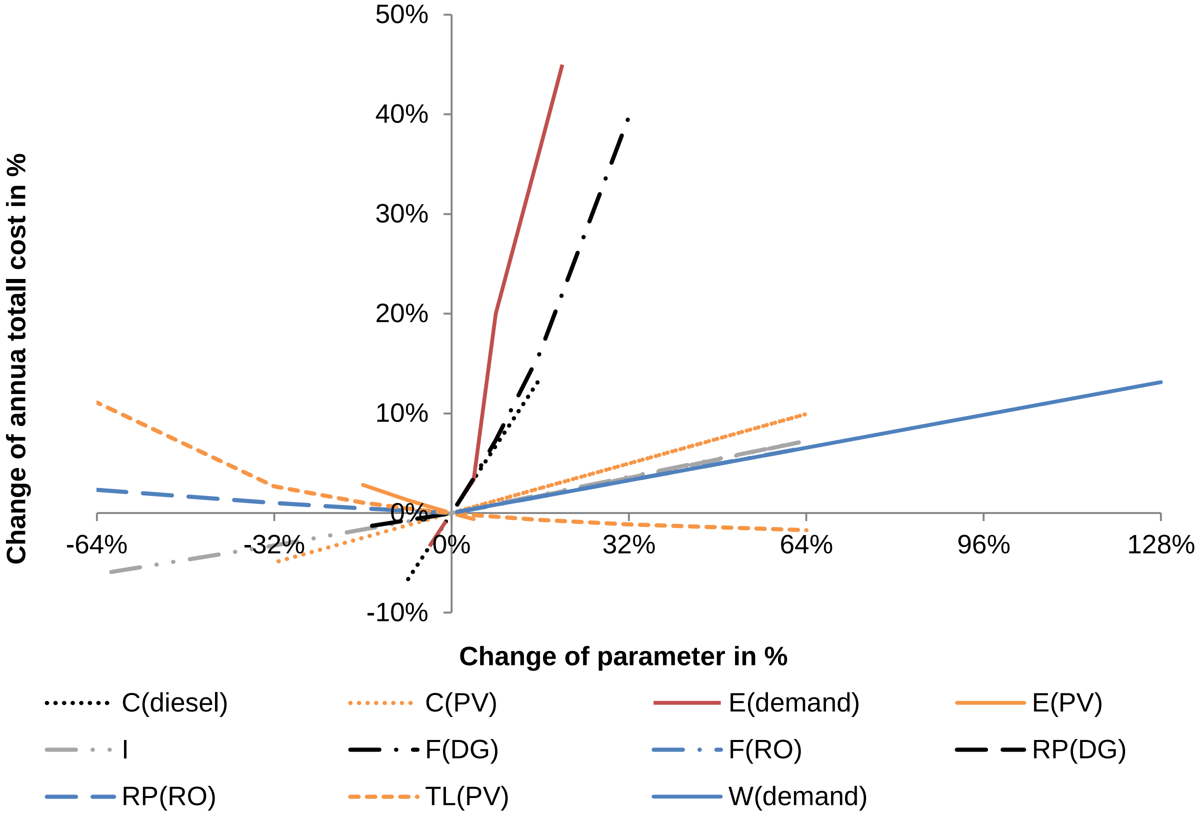

Fig. 15 Influence of the uncertain parameters on the annual costs

However, the rating of the importance of the uncertain parameters results of the maximal possible deviation of the total annual costs and is presented in Table 17. The electrical demand and the specific fuel consumption are by far the most important uncertain parameters, due to their high influence on the total costs. The price for the diesel fuel is ranked third, because of its comparatively lower uncertainty. The water demand, the life time of the PV system and the cost for the PV system follow closely on the next ranks. The interest factor and the specific energy consumption of the RO system still show an influence of more than 5% on the total costs, while the rated power of the DG and RO system as well as the degradation of the PV system and uncertainty of the solar irradiation can be neglected in comparison to the other parameters.

Table 17 Maximal absolute deviation of the total costs and ranking of the uncertain parameters

Parameter	Maximal absolute deviation of the annual total costs	Ranking of the importance of the parameter
$\mathbf{C^{diesel}}$	13.5%	3.
$\mathbf{C^{PV}}$	10.0%	6.
$\sum \mathbf{E_t^{demand}}$	45.0%	1.
$\sum \mathbf{e_t^{PV+DL}}$	2.8%	9.
$\mathbf{F^{DG,A}}$	39.7%	2.
$\mathbf{F^{RO}}$	6.7%	8.
$\mathbf{I}$	7.3%	7.
$\mathbf{LT^{PV}}$	11.1%	5.
$\mathbf{RP^{DG}}$	1.4%	11.
$\mathbf{RP^{RO}}$	2.3%	10.
$\sum \mathbf{W_t^{demand}}$	13.1%	4.

5.7 Limitations and disadvantages of the optimization model

Mathematical models cannot fully describe reality. One of the main limitations of the developed model is that no operating and maintenance costs are implemented. Furthermore, no electricity grid and no corresponding costs are modeled. Another limitation is the fact that the analyzed isolated grid, especially its DG, is seen as fixed without any possibilities to invest in a smaller or larger DG. Moreover, the model regards only one generic standard year for the electrical demand and the solar irradiation, which is used to analyze a time period of 20 years. Although deviations of the uncertain parameters are analyzed in chapter 5.6, the system parameters are assumed as constant during the time period. In order to limit the computational effort, one needs to alternate between the lp and the milp models, especially for studies of the BS. Because of the computational effort due to the milp model, additional optimizations to study the BS have not been realized.

6 Conclusion

The goal and motivation of this thesis is to answer the economic and functional interaction of PV power generation and flexible loads in isolated grids and the questions which are presented in chapter 1. In order to answer those issues, a mathematical optimization model for an isolated energy supply scenario has been developed and utilized for a case study of the remote islands of Lifuka and Foa in Tonga. As flexible loads, a desalination process in form of a RO system and a BS system are implemented and analyzed. For a better understanding of the model and its results, a sensitivity analysis, which includes an identification of the most important uncertain parameters, is conducted. The model is developed in GAMS as strictly lp, respectively milp and solved with IBMS`s Cplex solver.

The integration of PV power in an isolated grid results in lower costs for the energy supply. In the analyzed scenario a cost saving of 6% is achieved. The maximal electricity generation of the optimal PV system is even exceeding the actual electricity demand, which leads to a curtailment of PV power. In average, 7% of the generated PV power is not used. The additional integration of flexible loads is resulting in a better utilization of an existing PV system. The curtailed PV power is decreasing to 1%. This leads to a higher share of consumed PV power and to a reduction of the total costs by 1%. With the introduction of a flexible load, a higher PV capacity is economically preferable. Thus, the penetration of PV power can be enhanced further and the total costs can be decreased by 2%. The optimal PV capacity and the percentage of curtailed PV power are depending on the capacity of the flexible load and in particular on its degree of flexibility. In this thesis, the degree of freedom is analyzed as effective working time of the RO system. Although the actual implementation of the considered flexible operating RO system is economically not beneficial, it is shown that flexible loads in general are beneficial to increase the penetration of PV power. Furthermore, the results show that the analyzed BS system is disadvantageous compared to the RO system as flexible load, because of its charging and discharging losses. It is very surprising that the decentral integration of a flexible load with a price signal results in nearly the same key figures for the energy supply system compared to the optimization of the entire system. A simple forecast algorithm can be used to control the operation of the flexible load and a cheap integration of flexible loads could be realized by using the electricity frequency for transmitting the price signal, as presented in chapter 2.1.3. Thus, making the integration of available flexible loads preferable to investments in BS systems. However, it must be recognized that the integration of a single flexible load in this thesis is a simple and constructed case. The most important uncertain parameters in respect to the emerging total costs of the optimized energy supply system are related to the usage and operation of the DG. The electricity demand, the efficiency of the DG and the diesel fuel price are by far the most influencing and also the most important uncertain parameters.

Various possibilities for future research are seen in further studies of flexible loads and BS in isolated grids towards a higher penetration of renewable energies. The integration of other renewable resources like wind power are essential and are complementing PV power generation. Additional analysis of the BS system, especially in the context of taking over responsibility for the grid stability and realizing a DG shut-down, are necessary. A very broad and groundbreaking field of research opens up with the decentralized integration of flexible loads. In future research, it is essential to study the integration of multiple flexible loads instead of just a single one. A differentiation with several restrictions and several degrees of flexibility for the multiple flexible loads are desirable, in order to analyze their influence on the entire system and especially their interrelation between each other.

Bibliography

Abedi, S., Alimardani, A., Gharehpetian, G. B., Riahy, G. H., & Hosseinian, S. H. (2012). A comprehensive method for optimal power management and design of hybrid RES-based autonomous energy systems. *Renewable and Sustainable Energy Reviews, 16*(3), 1577-1587. doi: 10.1016/j.rser.2011.11.030

Akinyele, D. O., & Rayudu, R. K. (2014). Review of energy storage technologies for sustainable power networks. *Sustainable Energy Technologies and Assessments, 8*(0), 74-91. doi: 10.1016/j.seta.2014.07.004

Al-Shamma'a, A. A., & Addoweesh, K. E. (2012). Optimum sizing of hybrid PV/wind/battery/diesel system considering wind turbine parameters using Genetic Algorithm. 121-126. doi: 10.1109/PECon.2012.6450190

Alharbi, W., & Bhattacharya, K. (2013). Demand response and energy storage in MV islanded microgrids for high penetration of renewables. 1-6. doi: 10.1109/epec.2013.6802928

Amer, M., Namaane, A., & M'Sirdi, N. K. (2013). Optimization of Hybrid Renewable Energy Systems (HRES) Using PSO for Cost Reduction. *Energy Procedia, 42*(0), 318-327. doi: 10.1016/j.egypro.2013.11.032

Arul, P. G., Ramachandaramurthy, V. K., & Rajkumar, R. K. (2015). Control strategies for a hybrid renewable energy system: A review. *Renewable and Sustainable Energy Reviews, 42*(0), 597-608. doi: 10.1016/j.rser.2014.10.062

Asensio, M., & Contreras, J. (2014). Impact of demand response in an isolated system with high PV penetration. 1-6. doi: 10.1109/upec.2014.6934605

Bajpai, P., & Dash, V. (2012). Hybrid renewable energy systems for power generation in stand-alone applications: A review. *Renewable and Sustainable Energy Reviews, 16*(5), 2926-2939. doi: 10.1016/j.rser.2012.02.009

Bala, B. K., & Siddique, S. A. (2009). Optimal design of a PV-diesel hybrid system for electrification of an isolated island—Sandwip in Bangladesh using genetic algorithm. *Energy for Sustainable Development, 13*(3), 137-142. doi: 10.1016/j.esd.2009.07.002

Barbato, A., Capone, A., Chen, L., Martignon, F., & Paris, S. (2015). A distributed demand-side management framework for the smart grid. *Computer Communications, 57*(0), 13-24. doi: 10.1016/j.comcom.2014.11.001

Bognar, K. (2013). *Energy and water supply systems in remote regions considering renewable energies and seawater desalination*: Shaker.

Bognar, K., Blechinger, P., & Behrendt, F. (2012). Seawater desalination in micro grids: an integrated planning approach. *Energy, Sustainability and Society, 2*(1), 14. doi: 10.1186/2192-0567-2-14

Bognar, K., Pohl, R., & Behrendt, F. (2013). Seawater reverse osmosis (SWRO) as deferrable load in micro grids. *Desalination and Water Treatment, 51*(4-6), 1190-1199. doi: 10.1080/19443994.2012.715093

Bussieck, M. R., & Meeraus, A. (2004). General algebraic modeling system (GAMS) *Modeling languages in mathematical optimization* (pp. 137-157): Springer.

Campolongo, F., Saltelli, A., & Cariboni, J. (2011). From screening to quantitative sensitivity analysis. A unified approach. *Computer Physics Communications, 182*(4), 978-988. doi: 10.1016/j.cpc.2010.12.039

Carmeli, M. S., Castelli-Dezza, F., Mauri, M., Marchegiani, G., & Rosati, D. (2012). Control strategies and configurations of hybrid distributed generation systems. *Renewable Energy, 41*, 294-305. doi: 10.1016/j.renene.2011.11.010

Castillo, A., & Gayme, D. F. (2014). Grid-scale energy storage applications in renewable energy integration: A survey. *Energy Conversion and Management, 87*(0), 885-894. doi: 10.1016/j.enconman.2014.07.063

Census of Population and Housing. (2013). Nuku'alofa, Tonga: Statistics Department, Tonga.

Chang, K.-H., & Lin, G. (2015). Optimal design of hybrid renewable energy systems using simulation optimization. *Simulation Modelling Practice and Theory, 52*(0), 40-51. doi: 10.1016/j.simpat.2014.12.002

Chattopadhyay, D. (1999). Application of general algebraic modeling system to power system optimization. *Power Systems, IEEE Transactions on, 14*(1), 15-22.

Chauhan, A., & Saini, R. P. (2014). A review on Integrated Renewable Energy System based power generation for stand-alone applications: Configurations, storage options, sizing methodologies and control. *Renewable and Sustainable Energy Reviews, 38*, 99-120. doi: 10.1016/j.rser.2014.05.079

Climate Summary of Tonga. (2015) Retrieved 08.10.2015, from http://www.infrastructure.gov.to/meteorology/services/climate-information

CLIMATOLOGICAL INFORMATION – SALOTE PILOLEVU AIRPORT (HAP). (2006) Retrieved 08.10.2015, from http://www.met.gov.to/index_files/haapai.pdf

de Groot, M., Forbes, J., & Nikolic, D. (2013). Demand response in Isolated Power Systems. 1-6. doi: 10.1109/aupec.2013.6725443

Dietrich, K., Latorre, J. M., Olmos, L., & Ramos, A. (2012). Demand Response in an Isolated System With High Wind Integration. *IEEE Transactions on Power Systems, 27*(1), 20-29. doi: 10.1109/tpwrs.2011.2159252

ENERCON DESALINATION SYSTEMS. Retrieved 08.10.2015, from http://www.adu-res.org/pdf/Enercon.pdf

Fan, Y., Rimali, V., Tang, M., & Nayar, C. (2012). Design and Implementation of stand-alone smart grid employing renewable energy resources on Pulau Ubin Island of Singapore. 441-444. doi: 10.1109/apemc.2012.6237907

Fathima, A. H., & Palanisamy, K. (2015). Optimization in microgrids with hybrid energy systems – A review. *Renewable and Sustainable Energy Reviews, 45*(0), 431-446. doi: 10.1016/j.rser.2015.01.059

Finau, A. a. M. (2014). INTERNATIONAL MERCHANDISE TRADE STATISTICS. Nuku'alofa, Tonga: STATISTICS DEPARTMENT TONGA

Finn, P., & Fitzpatrick, C. (2014). Demand side management of industrial electricity consumption: Promoting the use of renewable energy through real-time pricing. *Applied Energy, 113*(0), 11-21. doi: 10.1016/j.apenergy.2013.07.003

Gantenbein, D., Binding, C., Jansen, B., Mishra, A., & Sundstrom, O. (2012). *EcoGrid EU: An efficient ICT approach for a sustainable power system.* Paper presented at the Sustainable Internet and ICT for Sustainability (SustainIT), 2012.

Gelazanskas, L., & Gamage, K. A. A. (2014). Demand side management in smart grid: A review and proposals for future direction. *Sustainable Cities and Society, 11*(0), 22-30. doi: 10.1016/j.scs.2013.11.001

Gellings, C. W. (1985). The concept of demand-side management for electric utilities. *Proceedings of the IEEE, 73*(10), 1468-1470. doi: 10.1109/proc.1985.13318

Hazelton, J., Bruce, A., & MacGill, I. (2014). A review of the potential benefits and risks of photovoltaic hybrid mini-grid systems. *Renewable Energy, 67*, 222-229. doi: 10.1016/j.renene.2013.11.026

Journeay-Kaler, P., & Mofor, L. (2013). Hybrid power systems. Abu Dhabi, United Arab Emirates: International Renewable Energy Agency (IRENA).

Kaabeche, A., & Ibtiouen, R. (2014). Techno-economic optimization of hybrid photovoltaic/wind/diesel/battery generation in a stand-alone power system. *Solar Energy, 103*(0), 171-182. doi: 10.1016/j.solener.2014.02.017

Kaldellis, J. K., Zafirakis, D., & Kondili, E. (2010). Optimum sizing of photovoltaic-energy storage systems for autonomous small islands. *International Journal of Electrical Power & Energy Systems, 32*(1), 24-36. doi: 10.1016/j.ijepes.2009.06.013

Käufler, J., Pohl, R., & Sader, H. (2012). Seawater desalination (RO) as a wind powered industrial process — Technical and economical specifics. *Desalination and Water Treatment, 31*(1-3), 359-365. doi: 10.5004/dwt.2011.2347

Krajačić, G., Duić, N., & Carvalho, M. d. G. (2009). H2RES, Energy planning tool for island energy systems – The case of the Island of Mljet☆. *International Journal of Hydrogen Energy, 34*(16), 7015-7026. doi: 10.1016/j.ijhydene.2008.12.054

L. A. C. Lopes, Katiraei, F., Mauch, K., Vandenbergh, M., & Arribas, L. (2012). PV Hybrid Mini-Grids: Applicable Control Methods for Various Situations: INTERNATIONAL ENERGY AGENCY.

Livengood, D., Sim-Sim, F. C., Ioakimidis, C. S., & Larson, R. (2010). Responsive demand in isolated energy systems. *1*, 197-207. doi: 10.2495/islands100171

Lund, P. D., Lindgren, J., Mikkola, J., & Salpakari, J. (2015). Review of energy system flexibility measures to enable high levels of variable renewable electricity. *Renewable and Sustainable Energy Reviews, 45*(0), 785-807. doi: 10.1016/j.rser.2015.01.057

Luo, Y., Shi, L., & Tu, G. Y. (2014). Optimal sizing and control strategy of isolated grid with wind power and energy storage system. *Energy Conversion and Management, 80*, 407-415. doi: 10.1016/j.enconman.2014.01.061

Mahlia, T. M. I., Saktisahdan, T. J., Jannifar, A., Hasan, M. H., & Matseelar, H. S. C. (2014). A review of available methods and development on energy storage; technology update. *Renewable and Sustainable Energy Reviews, 33*(0), 532-545. doi: 10.1016/j.rser.2014.01.068

Mathioulakis, E., Belessiotis, V., & Delyannis, E. (2007). Desalination by using alternative energy: Review and state-of-the-art. *Desalination, 203*(1-3), 346-365. doi: 10.1016/j.desal.2006.03.531

Mofor, L., Isaka, M., Wade, H., & Soakai, A. (2013). Pacific Lighthouses: Renewable Energy Roadmapping for Islands: International Renewable Energy Agency (IRENA).

Mohammed, Y. S., Mustafa, M. W., & Bashir, N. (2014). Hybrid renewable energy systems for off-grid electric power: Review of substantial issues. *Renewable and Sustainable Energy Reviews, 35*(0), 527-539. doi: 10.1016/j.rser.2014.04.022

. National Integrated Water Resource Management Diagnostic Report: Tonga. (2007): South Pacific Applied Geoscience Commission (SOPAC).

Nayar, C., Markson, T., & Suponthana, W. (2008). Wind/PV/diesel micro grid system implemented in remote islands in the Republic of Maldives. 1076-1080. doi: 10.1109/icset.2008.4747166

Nehrir, M. H., Wang, C., Strunz, K., Aki, H., Ramakumar, R., Bing, J., . . . Salameh, Z. (2011). A Review of Hybrid Renewable/Alternative Energy Systems for Electric Power Generation: Configurations, Control, and Applications. *Ieee Transactions on Sustainable Energy, 2*(4), 392-403. doi: 10.1109/Tste.2011.2157540

Nema, P., Nema, R. K., & Rangnekar, S. (2009). A current and future state of art development of hybrid energy system using wind and PV-solar: A review. *Renewable and Sustainable Energy Reviews, 13*(8), 2096-2103. doi: 10.1016/j.rser.2008.10.006

Neves, D., Silva, C. A., & Connors, S. (2014). Design and implementation of hybrid renewable energy systems on micro-communities: A review on case studies. *Renewable and Sustainable Energy Reviews, 31*(0), 935-946. doi: 10.1016/j.rser.2013.12.047

Nikolic, D., Negnevitsky, M., de Groot, M., Gamble, S., Forbes, J., & Ross, M. (2014). Fast demand response as an enabling technology for high renewable energy penetration in isolated power systems. 1-5. doi: 10.1109/pesgm.2014.6939282

Novosel, T., Ćosić, B., Krajačić, G., Duić, N., Pukšec, T., Mohsen, M. S., . . . Ababneh, A. K. (2014). The influence of reverse osmosis desalination in a combination with pump storage on the penetration of wind and PV energy: A case study for Jordan. *Energy, 76*, 73-81. doi: 10.1016/j.energy.2014.03.088

O׳Connell, N., Pinson, P., Madsen, H., & O׳Malley, M. (2014). Benefits and challenges of electrical demand response: A critical review. *Renewable and Sustainable Energy Reviews, 39*(0), 686-699. doi: 10.1016/j.rser.2014.07.098

Osterwald, C. R., Anderberg, A., Rummel, S., & Ottoson, L. (2002). Degradation analysis of weathered crystalline-silicon PV modules. 1392-1395. doi: 10.1109/pvsc.2002.1190869

Papapetrou, M., Wieghaus, M., & Biercamp, C. (2010). *Roadmap for the development of desalination powered by renewable energy*: Frauenhofer Verlag.

Paulsen, K., & Hensel, F. (2007). Design of an autarkic water and energy supply driven by renewable energy using commercially available components. *Desalination, 203*(1-3), 455-462. doi: 10.1016/j.desal.2006.04.021

Peñate, B., Castellano, F., Bello, A., & García-Rodríguez, L. (2011). Assessment of a stand-alone gradual capacity reverse osmosis desalination plant to adapt to wind power availability: A case study. *Energy, 36*(7), 4372-4384. doi: 10.1016/j.energy.2011.04.005

Pina, A., Silva, C., & Ferrão, P. (2012). The impact of demand side management strategies in the penetration of renewable electricity. *Energy, 41*(1), 128-137. doi: 10.1016/j.energy.2011.06.013

Pohl, R., Kaltschmitt, M., & Holländer, R. (2009). Investigation of different operational strategies for the variable operation of a simple reverse osmosis unit. *Desalination, 249*(3), 1280-1287. doi: 10.1016/j.desal.2009.06.029

Ramchurn, S. D., Vytelingum, P., Rogers, A., & Jennings, N. (2011). *Agent-based control for decentralised demand side management in the smart grid.* Paper presented at the The 10th International Conference on Autonomous Agents and Multiagent Systems-Volume 1.

Ramos, F., Canizares, C., & Bhattacharya, K. (2014). Effect of price responsive demand on the operation of microgrids. 1-7. doi: 10.1109/pscc.2014.7038312

Rious, V., & Perez, Y. (2014). Review of supporting scheme for island powersystem storage. *Renewable and Sustainable Energy Reviews, 29*, 754-765. doi: 10.1016/j.rser.2013.08.015

Saltelli, A., & Annoni, P. (2010). How to avoid a perfunctory sensitivity analysis. *Environmental Modelling & Software, 25*(12), 1508-1517. doi: 10.1016/j.envsoft.2010.04.012

Schäfer, B., Matthiae, M., Timme, M., & Witthaut, D. (2015). Decentral Smart Grid Control. *New Journal of Physics, 17*(1), 015002. doi: 10.1088/1367-2630/17/1/015002

Schies, A. (2013). *Technological and economic assesssment of PV-Diesel hybrid solutions versus other technologies*. Paper presented at the PEP Information Workshop:PV-Hybrid Systems in Indonesia, Berlin.

Schweppe, F. C. (1982). Frequency adaptive, power-energy re-scheduler: Google Patents.

Schweppe, F. C., Caramanis, M. C., Tabors, R. D., & Bohn, R. E. (1988). *Spot pricing of electricity*: Springer Science & Business Media.

Segurado, R., Costa, M., Duić, N., & Carvalho, M. G. (2015). Integrated analysis of energy and water supply in islands. Case study of S. Vicente, Cape Verde. *Energy*. doi: 10.1016/j.energy.2015.02.013

Segurado, R., Krajačić, G., Duić, N., & Alves, L. (2011). Increasing the penetration of renewable energy resources in S. Vicente, Cape Verde. *Applied Energy, 88*(2), 466-472. doi: 10.1016/j.apenergy.2010.07.005

Setiawan, A. A., Zhao, Y., & Nayar, C. V. (2009). Design, economic analysis and environmental considerations of mini-grid hybrid power system with reverse osmosis desalination plant for remote areas. *Renewable Energy, 34*(2), 374-383. doi: 10.1016/j.renene.2008.05.014

Sharafi, M., & Elmekkawy, T. Y. (2014). Multi-objective optimal design of hybrid renewable energy systems using PSO-simulation based approach. *Renewable Energy, 68*(0), 67-79. doi: 10.1016/j.renene.2014.01.011

Shariatzadeh, F., Mandal, P., & Srivastava, A. K. (2015). Demand response for sustainable energy systems: A review, application and implementation strategy. *Renewable and Sustainable Energy Reviews, 45*(0), 343-350. doi: 10.1016/j.rser.2015.01.062

Short, J. A., Infield, D. G., & Freris, L. L. (2007). Stabilization of Grid Frequency Through Dynamic Demand Control. *IEEE Transactions on Power Systems, 22*(3), 1284-1293. doi: 10.1109/tpwrs.2007.901489

SMA FUEL SAVE CONTROLLER. Retrieved 05.10.2015, 2015, from http://files.sma.de/dl/26900/FSCM-DEN1531-V21web.pdf

Subramani, A., Badruzzaman, M., Oppenheimer, J., & Jacangelo, J. G. (2011). Energy minimization strategies and renewable energy utilization for desalination: a review. [Research Support, Non-U.S. Gov't Review]. *Water Res, 45*(5), 1907-1920. doi: 10.1016/j.watres.2010.12.032

Swales, M., Hughes, W., & Asseline, F. (2010). Electric Supply System Load Forecast: Kingdom of Tonga. Washington, DC 20433 USA: The World Bank Group.

TONGA ENERGY ROAD MAP (TERM) 2010-2020. (2010). Tonga: His Majesty's Government of the Kingdom of Tonga.

Tsutsumi, A. (Producer). (2012). Retrieved from http://www.u-tokyo.ac.jp/content/400021988.jpg

Tzen, E., & Papapetrou, M. (2012). Promotion of renewable energy sources for water production through desalination. *Desalination and Water Treatment, 39*(1-3), 302-307. doi: 10.1080/19443994.2012.669232

Upadhyay, S., & Sharma, M. P. (2014). A review on configurations, control and sizing methodologies of hybrid energy systems. *Renewable & Sustainable Energy Reviews, 38*, 47-63. doi: 10.1016/j.rser.2014.05.057

Upadhyay, S., & Sharma, M. P. (2015). Development of hybrid energy system with cycle charging strategy using particle swarm optimization for a remote area in India. *Renewable Energy, 77*(0), 586-598. doi: 10.1016/j.renene.2014.12.051

Walter, T. (2014). *Smart Micro Grids and the Easy Smart Grid Approach* Paper presented at the Workshop and Symposium „Future Energy Systems“, Göttingen.

Wang, R., Wang, P., Xiao, G., & Gong, S. (2014). Power demand and supply management in microgrids with uncertainties of renewable energies. *International Journal of Electrical Power & Energy Systems, 63*(0), 260-269. doi: 10.1016/j.ijepes.2014.05.067

Wang, X., Palazoglu, A., & El-Farra, N. H. (2015). Operational optimization and demand response of hybrid renewable energy systems. *Applied Energy, 143*(0), 324-335. doi: 10.1016/j.apenergy.2015.01.004

Werner, C., & Breyer, C. (2012). *Analysis of mini-grid installations: an overview on system configurations.* Paper presented at the 27th European photovoltaic solar energy conference and exhibition, Frankfurt.

Xueshu, C., Lapthorn, A., & Peimankar, A. (2014). An isolated hybrid renewable energy system: Ha'apai island group in the Kingdom of Tonga. 102-107. doi: 10.1109/icpere.2014.7067240

Yamegueu, D., Azoumah, Y., Py, X., & Zongo, N. (2011). Experimental study of electricity generation by Solar PV/diesel hybrid systems without battery storage for off-grid areas. *Renewable Energy, 36*(6), 1780-1787. doi: 10.1016/j.renene.2010.11.011

Yang, H., Lu, L., & Zhou, W. (2007). A novel optimization sizing model for hybrid solar-wind power generation system. *Solar Energy, 81*(1), 76-84. doi: 10.1016/j.solener.2006.06.010

Yekini Suberu, M., Wazir Mustafa, M., & Bashir, N. (2014). Energy storage systems for renewable energy power sector integration and mitigation of intermittency. *Renewable and Sustainable Energy Reviews, 35*(0), 499-514. doi: 10.1016/j.rser.2014.04.009

Appendix

A Background

Table 18 System sizing and energy management approaches for an isolated hybrid grid

Author	Focus	Components	Objective	Optimization approach	Case study
Yang, Lu, and Zhou (2007)	Sizing	Solar, Wind, Battery	LCOE, loss of power supply probability	Iterative process	Island in China
Nayar, Markson, and Suponthana (2008)	System planning	Solar, Wind, Battery, Diesel	LCOE, fuel saved, initial capital requirements	HOMER	Maldives
Bala and Siddique (2009)	Optimal design	Solar, battery, Diesel	Initial costs, operation and maintenance costs	Genetic algorithm	Island in Bangladesh
Krajačić, Duić, and Carvalho (2009)		Renewables, fossils, storages, deferrable loads, hydrogen loop	Penetration of renewables	H2RES	Island in Croatia
Kaldellis, Zafirakis, and Kondili (2010)	Sizing of PV and storage for autonomous energy supply	Solar, storages, diesel	LCOE	Iterative process (Variation of PV peak power and energy autonomy)	Greek island
Abedi, Alimardani, Gharehpetian, Riahy, and Hosseinian (2012)	Sizing and power management strategy	Wind, solar, storages	Overall cost, unmet load, fuel emissions	Differential Evolution algorithm	Ardebil city, Iran
Al-Shamma'a and Addoweesh (2012)	Sizing	Wind, solar, battery, diesel	LCOE	Genetic algorithms	Village, Saudi arabia
Amer, Namaane, and M'Sirdi (2013)	Sizing	Wind, Solar, Battery, Diesel	LCOE	Particle swarm optimization	Household
Kaabeche and Ibtiouen (2014)	Sizing and energy management		Total energy deficit, total net present cost, energy cost	Iterative process	Ghardaia, Algeria
Luo, Shi, and Tu (2014)	Storage sizing with wind power	Wind, Storage	Annualized costs	Genetic algorithm	Island, China
Sharafi and Elmekkawy (2014)	Sizing	Wind, solar, diesel, batteries, fuel cell, electrolyzer, hydrogen tank	Total costs, unmet load, fuel emission	Particle swarm optimization	Zaragoza, Spain

R. Wang, Wang, Xiao, and Gong (2014)	Energy management with uncertainty of renewables as probability function	Wind, Solar, Conventional Generators	Variable costs (fuel consumed)		
Xueshu, Lapthorn, and Peimankar (2014)	Sizing	Wind, Solar, Battery, Diesel	Annualized system cost, annualized capital cost LCOE),net present cost	HOMER	Ha´apai, Tonga
Chang and Lin (2015)	Sizing of several power stations	Wind, Solar, Battery, Diesel, Storages	Total costs (considering allocation and transmission)	Metamodel-based algorithm	
Subho Upadhyay and Sharma (2015)	Sizing and energy management strategy	Wind, Solar, Biomass/biogas, Battery, Diesel	LCOE	Particle swarm optimization	Villages, India
X. Wang, Palazoglu, and El-Farra (2015)	Sizing and energy management	Wind, Solar, Battery, Diesel	Annual capital cost	Iterative process based on total energy demand and production; Dynamic simulation with minimization on total costs based on energy flows	Household, California

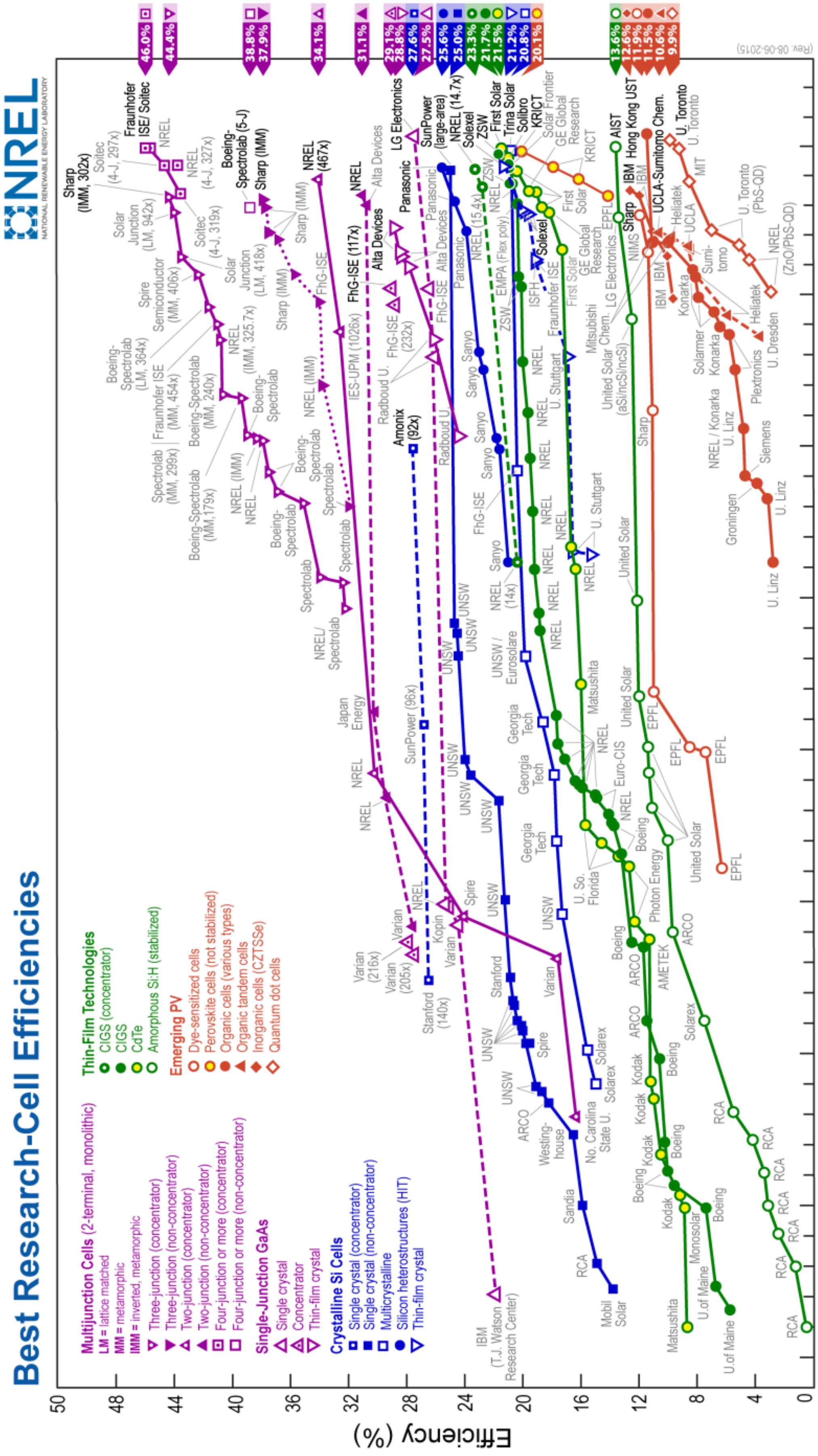

Fig. 16 Development of different PV technologies Photovoltaics (2015)

B Model script of the developed lp

```
*model for the optimization of PV+BS size and control of the isolated grid
Sets
t time steps in 15 min for a whole year /1*35040/
h  time steps in 1h for a whole year /1*8760/    ;

Parameter
PVhelp(h)   normalized supply of PV in kWh
PVdeltahelp(h) delta of normalized irradation
ePV1kWP(t)
Edemand(t)    static demand of Tonga in kWh
Wdemand(t)    water demand of Tonga in liter;

*from excel data spreadsheet to gdx input files
*$call "gdxxrw PV_tonga.xlsx o=PV_tonga.gdx @PVin.txt"
*$call "gdxxrw DE_tonga.xlsx o=DE_tonga.gdx @DEin.txt"
*$call "gdxxrw DW_tonga.xlsx o=DW_tonga.gdx @DWin.txt"

*load data from gdx input files to the model
$gdxin PV_tonga.gdx
$load PVhelp
$gdxin

$gdxin DE_tonga.gdx
$load DE
$gdxin

$gdxin DW_tonga.gdx
$load DW
$gdxin

*interpolation of PV data to 15 minutes steps
PVdeltahelp(h) = PVhelp(h++1) - PVhelp(h)
loop(h,
```

```
PV1kWP(t)$(ord(t) <= ord(h)*4 and ord(t)>(ord(h)-1)*4) = PVhelp(h) + PVdeltahelp(h)/4 * (ord(t)-((ord(h)-1)*4+1));)


Scalar
Cdiesel     price of one liter of diesel ($ per l)                /1.2/
FDGa        factor a for the DG (l per kWh)                       /0.25/
FDGb        factor b for the DG (l per kWh)
FDGc        factor c for the DG (l per kW)
LDG         additional consumption for low loading                /0.3/
RPDG         rated power of diesel generator (kW)                 /372/
FRO         working efficiency of RO system (kWh per m³)   /2.5/
RPRO        rated power of reverse osmosis system (kW)            /36.485/
LRO         infinitesimal loss factor for RO                      /0.0001/
SWSmax      maximal WS (days)                               /2/
CPV         price of one kW of peak power ($ per pkW)       /2500/
CBS         price of one BS unit                            /1200/
EBScap      power per BS unit (kW)                                /1/
SBScap       energy capacity per BS unit (kWh)              /1/
LBSrte       charging and discharging losses of BS                /0.1/
LBSdd       maximal discharge level of BS                         /0.9/
I           interest rate                                         /0.1/
ANFPV       annuity factor for PV
ANFBS       annuity factor for BS
TLPV        operating life of PV station                    /20/
TLBS        operating life of BS                                  /10/
;

Variables
costtotal
eBS(t)      BS charge and discharge
;

Positive variables
diesel(t) consumption of diesel per time step in liter
eDG(t)      energy output of the diesel generator
```

ePV(t)	*consumed PV power*
sWS(t)	*water storage*
costPV	*costs for PV*
capacityPV	*peak power of PV system*
wRO(t)	*water inflow of RO to water storage*
costBS	*cost of BS*
eBSpos(t)	*charging of BS*
eBSneg(t)	*discharging of BS*
gBS(t)	*auxiliary variable of B Sfor grid stability*
capacityBS	*number of units of BS*
eRO (t)	*reverse osmosis power demand*
eROpos (t)	*auxiliary variables for reverse osmosis power demand*
eRO neg(t)	*reverse osmosis power demand*
eDL(t)	*dump load of PV*

;

Equations

cost	*objective function with annulized costs in $*
water(t)	*water equations for water storage and input*
waterelectric(t)	*relation from water input to reverse osmosis electric demand*
ROchange(t)	*determining the change of RO demand*
dieselelectric1(t)	*relation from consumed diesel to energy input in grid*
pvgeneration(t)	*determining the usage of PV power*
grid(t)	*grid equation for balancing electrical demand and supply*
investPV	*investement for PV*
investBS	*investemnt for the lihtium battery*
gridrestriction(t)	*restriction for a minimal energy supply by diesel generator*
batterygridenergy(t)	*restriction for battery grid stabilistation in regard to SOC*
batterygridpower(t)	*restriction for battery grid stabilistation in regard to power output*
battery(t)	*battery equation for charging discharging and storage*
batteryinoutlosses(t)	*losses for charging discharging*
energybattery(t)	*restriction for eneryg capacity regarding investment*
powerbattery(t)	*restriction for charging and discharging power regarding investment*

;

```
*equation for electric demand and supply
grid(t).. Edemand(t) + eRO(t) =e= ePV(t) + eDG(t) +eBS(t) ;

*diesel generator
FDGc = (LDG/FDGa)/(7);
FDGb = FDGa - FDGc;
dieselelectric(t).. diesel(t) =e=   eDG(t)*FDGb + RPDG/4*FDGc ;
eDG.up(t) = RPdiesel/4;

*PV power generation
pvgeneration(t).. ePV(t) =e= ePV1kWP(t)*capacityPV/4 - eDL(t);

* reverse osmosis system
waterelectric(t).. eRO(t) =e= wRO(t) *  FRO + eROpos(t)*LRO ;
wRO(t).up =  RPRO*2/FRO/4;
ROchange(t).. eRO(t--1) - eRO(t) =e= eROpos(t) - eROneg(t);

*model for water tank
water(t).. sWS(t) =e= sWS(t--1) + wRO(t) - Wdemand(t);
sWS(t).up = sum(t,DW(t))/(card(t)/96)*SWSmax;

*cost for PV
investPV..  costPV =e= CPV * capacityPV * ANFpv;

*cost for BS
investBLI.. costBS =e= CBS * capacityBS * ANFbs;

*BS
battery (t).. sBS(t) =e= sBS(t--1) - eBS(t) - eBSpos(t)*effLI;
batteryinoutlossesLI(t).. eBS(t) =e= eBSpos(t) - eBSneg(t);
energybattery(t).. sBS(t) =l= SBScap * capacityBS;
powerbattery (t).. eBS(t) =l= EBScap/4 * capacityBS;
```

```
*grid stability
gridrestriction(t).. gBS(t)/16+DG1(t) =g=  RPdiesel/8;
batterygridenergy(t).. gBS(t) =l= sBS(t);
batterygridpower(t).. gBS(t) =l= EBScap * capacityBS;

*annuity factors
ANFpv = ((1+i)**TLPV)*i/(((1+i)**TLPV)-1);
ANFli = ((1+i)**TLBS)*i/(((1+i)**TLBS)-1);

*total cost
cost.. costtotal =e= sum(t, diesel(t)) * Cdiesel + costPV + costBS/LBSdd;


Model Tonga      /all/


Solve Tonga using lp minimizing costtotal;
```